ACS Partner Journal

CHEM & BIO ENGINEERING

pubs.acs.org/ChemBioEng

Review

Recent Progress of Halide Redox Mediators in Lithium−Oxygen Batteries: Functions, Challenges, and Perspectives

Kang Huang, Zhixiu Lu, Shilong Dai, and Huilong Fei*

Cite This: *Chem Bio Eng.* 2024, 1, 737−756

Read Online

ACCESS | Metrics & More | Article Recommendations

ABSTRACT: Lithium−oxygen batteries (LOBs) have received much research interest owing to their ultra-high energy density, but their further development is restricted by the erosion of the Li anode, the degradation of the electrolyte, and especially the sluggish oxygen-involving reactions on the cathode. To facilitate the oxidation of discharge products, halide redox mediators (HRMs), a subclass of soluble additives, have been explored to promote their decomposition. Meanwhile, some other intriguing functions were discovered, like protecting the Li anode and redirecting the discharge pathway to form LiOH. In this Review, after a brief introduction of LOBs and HRMs, the various functions of HRMs, not limited to promoting the oxidation of discharge products, are discussed and summarized. In addition, the challenges and controversies confronted by HRMs in LOBs are highlighted and the future opportunities of HRMs for achieving better LOBs are proposed.

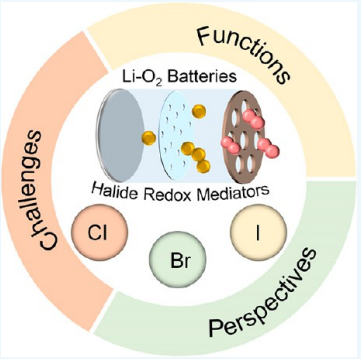

KEYWORDS: *homogenous catalysts, halide redox mediators, lithium−oxygen batteries, LiOH chemistry, versatile additives, shuttling effect*

1. INTRODUCTION

Growing concerns over the depletion of fossil fuels and damage to the environment call for clean energy storage technologies like rechargeable batteries.[1,2] Li-ion batteries (LIBs) have been the dominant power option in the past 30 years but are restricted by their low energy density (<300 Wh/kg) related to their intercalation chemistry.[3−5] Moving from intercalation chemistry to conversion chemistry, lithium−air batteries (LABs), also called lithium−oxygen batteries (LOBs) in the lab stage with pure O_2 as the reactant, have gained much attention owing to their high theoretical energy density (∼3500 Wh/kg), making them promising alternatives to conventional LIBs.[6−9] However, currently, several critical issues associated with the Li anode, the electrolyte, and especially the air cathode of LOBs have been puzzling.[10−14] As a result of the multi-electron-transfer reactions and the undesirable contact of insulating discharge products deposited on the cathode surface, the kinetics of the electro-oxidation of discharge products are sluggish, leading to large charge overpotentials.[15−17] The high potential as well as reactive oxygen intermediates (ROIs) formed during the charge process would incur severe side reactions and further cause poor cyclability and low energy efficiency of the system.[13,18−20]

To speed up the decomposition of discharge products, a special subclass of soluble additives, namely redox mediators (RMs), have played vital roles in facilitating the sluggish kinetics and enhancing the energy efficiency like solid catalysts.[17,21−24] Specifically, a RM is oxidized at the electrode surface, diffuses through the electrolyte to the surface of the discharge products, and reacts chemically with them, after which the oxidizing RM is reduced and the discharge products are decomposed gradually.[15] Compared with solid catalysts, the dissolved oxidizing species guarantees feasible contact with the solid deposits, regardless of their location, size, and structure, leading to a high oxidation efficiency and low charge potential.[25,26] In addition, the additive-aided oxidation of discharge products, taking Li_2O_2 for example, can circumvent the formation of ROIs and thus prevent the degradation of the electrolyte and cathode.[27,28] Having these advantages, along with their low cost and adjustable redox properties, RMs have become a hot research topic in the field of LOBs.[29]

Up to now, three types of RMs—organic (e.g., vitamin K1 and 2,2,6,6-tetramethylpiperidinyloxyl), organometallic (e.g., iron phthalocyanine and heme), and halide redox mediators (HRMs)—have been developed.[30−35] Among them, organic and organometallic RMs, even in their reduced state, are vulnerable to ROIs and the Li metal anode, while HRMs are relatively stable.[21] Besides, the molecule sizes of HRMs are generally much smaller than those of organic and organometallic RMs, enabling their faster diffusion.[36] Furthermore, the wide sources and the simple preparation of HRMs make them more attractive. Initially, Li halides (e.g., LiI and LiBr) were used as

Received: January 28, 2024
Revised: March 8, 2024
Accepted: March 17, 2024
Published: April 2, 2024

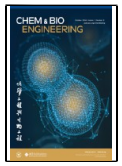

https://doi.org/10.1021/cbe.4c00025
Chem Bio Eng. 2024, 1, 737−756

the common charging RMs to promote the oxidation of Li_2O_2 discharge product.[25,37−40] Thereafter, the unique functions of Li halides, like inducing the generation of LiOH and the decomposition of side products, were discovered.[41,42] Subsequently, various HRMs were designed by replacing Li^+ with other organic cations.[43,44] So far, distinct performance enhancements of LOBs have been achieved by using HRMs, but some critical challenges and disputations are still present.

Some insightful reviews have summarized various RMs including HRMs, while the functions of HRMs were generalized partially and the mechanisms of HRM-involving LOBs were discussed sparsely.[21,24,27,29,45] In this Review, after a brief introduction of LOBs and HRMs, we systematically summarize various functions of HRMs (Figure 1), including the following:

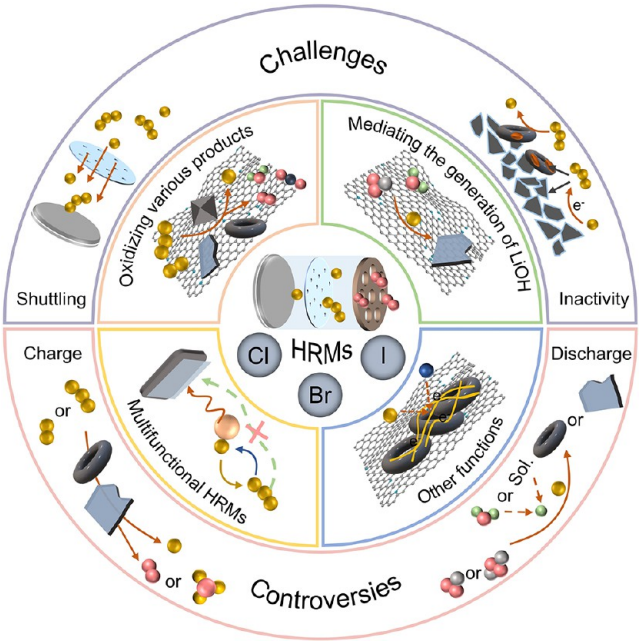

Figure 1. Overall picture of the research progress on HRMs in LOBs: functions, challenges, and controversies.

(i) their role as electron−hole carriers to promote the oxidation of Li_2O_2, LiOH, Li_2CO_3, and other related compounds; (ii) their ability to redirect the discharge pathway for generating LiOH; (iii) their multifunctional roles including protection of the Li anode, suppression of shuttling, and decomposition of discharge products; and (iv) other effects provided mainly by the Cl-based HRMs. Subsequently, the challenges like redox shuttling and inactivity of the oxidized HRMs and the controversies about the discharge/charge processes are highlighted. Finally, future opportunities for the development of HRMs are proposed for realizing better LOBs.

2. FUNDAMENTALS AND BASICS OF LOBs AND HRMs

2.1. Work Mechanisms and Challenges of LOBs. A typical aprotic LOB comprises a metallic Li anode, a separator soaked with electrolyte containing the organic solvent, Li salt, and additives, and a porous cathode loaded with catalysts (Figure 2a).[8] During discharge, the Li anode is oxidized to Li^+ ($Li^0 \rightarrow Li^+ + e^-$) and O_2 obtains two electrons from an external circuit and combines with Li^+ to form Li_2O_2 ($O_2 + 2e^- + 2Li^+ \rightarrow Li_2O_2$, oxygen reduction reaction (ORR)). During charge, Li_2O_2 is decomposed with the liberation of O_2 and Li^+ ($Li_2O_2 \rightarrow O_2 + 2e^- + 2Li^+$, oxygen evolution reaction (OER)) and Li^+ turns back to Li deposited on the surface of the Li anode ($Li^+ + e^- \rightarrow Li^0$).[46,47] Although the reactions between Li^+ and O_2 in LOB are simple as listed above, the detailed mechanism is rather complex and still under debate.[20,48−50] By virtue of some advanced techniques, several ROIs, including O_2^-, LiO_2, and $^1O_2$, were detected in both discharge and charge processes.[51−53] These ROIs, coupled with Li_2O_2, would attack the commonly used electrolytes and carbon-containing cathodes, causing the generation of multiple parasitic products and thus ultimately inducing low capacity and poor round-trip efficiency.[19,54−56] In addition, the oxidation of Li_2O_2 is sluggish because of its wide bandgap (4−5 eV) that further leads to a large charge overpotential, poor rate capability, and severe parasite reactions.[57−59] Furthermore, the active anode Li faced problems due to the growth of dendrites and the crossover of O_2, CO_2, H_2O, and so on, leading to a low Coulombic efficiency and energy density loss in LOBs.[11,60−62] To improve the performance of LOBs, strategies were concentrated on (i) accelerating the reaction kinetics by solid/liquid catalysts;[38,63] (ii) introducing special additives (e.g., H_2O and $^1O_2$ quencher) to lower the activity of ROIs;[19,64] (iii) converting the discharge product from Li_2O_2 to LiOH, LiO_2, or Li_2O;[41,65,66] and (iv) protecting the Li anode by stable solid electrolyte interface (SEI) layers or SEI-like films.[44] In these strategies, halide-based additives were often used to fulfill one or more goals for promoting the performance of LOBs.

2.2. Basics of HRMs. HRMs are a class of compounds comprising halogen anions (i.e., Cl^-, Br^-, and I^-) and metal cations (e.g., Li^+ and In^{3+}) or organic cations (e.g., $C_6H_{15}S^+$).

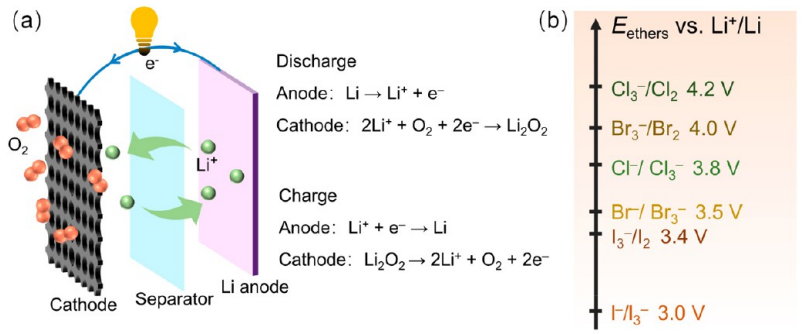

Figure 2. (a) Configuration and work mechanism of aprotic LOBs. (b) Redox potentials against the potential of Li^+/Li of $Cl^-/Cl_3^-/Cl_2$, $Br^-/Br_3^-/Br_2$, and $I^-/I_3^-/I_2$ in ether electrolyte.

https://doi.org/10.1021/cbe.4c00025
Chem Bio Eng. 2024, 1, 737−756

Table 1. Collection of Various HRMs Grouped by Their Functions and Their Battery Performances

HRMs	Electrolytes	Cathodes	Discharge products	Active species	Cycle performance	Ref
			Oxidizing Li_2O_2			
LiI (50 mM)	1.0 M LiTFSI/TEGDME	Carbon nanotube fibrils	Li_2O_2	I_3^-	900 cycles (1000 mAh/g at 2000 mA/g)	38
LiI (50 mM)	Gel electrolyte	Spinnable carbon nanotube	Li_2O_2	I_3^-	610 cycles (1000 mAh/g at 2000 mA/g)	67
LiBr (50 mM)	0.2 M LiTFSI/diglyme	Monolithic aerogel carbon paper	Li_2O_2	Br_3^-	40 cycles (0.52 mAh/cm^2 at 0.052 mA/cm^2)	37
			Oxidizing LiOH			
LiI (50 mM)	0.25 M LiTFSI/DME with H_2O	Reduced graphene oxide	LiOH	I_3^-	2000 cycles (1 Ah/g at 1 A/g)	41
LiI (0.2 M)	0.1 M LiTFSI/DME with 500 ppm of H_2O	Carbon black	LiOH	I_2	–	68
LiI (50 mM)	0.5 M LiTFSI/DME with 9.1 vol% H_2O	Carbon felt	LiOH and LiOOH	I_2	–	69
LiCl (50 mM)	0.45 M $LiClO_4$/DMSO	Hierarchical carbon nanocages	LiOH	Cl_3^-	71 cycles (500 mAh/g at 500 mA/g)	70
			Oxidizing Li_2CO_3			
LiBr (10 mM)	1.0 M LiTFSI/DME	Ketjenblack	Li_2O_2 with Li_2CO_3	Br_2	–	42
LiBr (0.4 M)	1.0 M LiTFSI/TEGDME	Multi-walled carbon nanotubes	Li_2CO_3	$Br_2\cdots Br_3^-$ complex	12 cycles (1000 mAh/g at 50 mA/g)	71
			Mediating the Generation of LiOH			
LiI (1.0 M)	LiI/TEGDME	Super P	LiOH	I^-	–	72
LiI (50 mM)	0.25 M LiTFSI/DME with H_2O	Reduced graphene oxide	LiOH	I^-	2000 cycles (1 Ah/g at 1 A/g)	41
LiI (1.0 M)	LiI/TEGDME	Ketjenblack	LiOH	I^-	–	73
LiI (0.2 M)	0.1 M LiTFSI/DME with 500 ppm of H_2O	Carbon black	LiOH	I^-	–	68
LiI (0.1 M)	0.2 M LiTFSI/DME with 1000 ppm of H_2O	Carbon nanotubes	LiOH	I^-	–	74
LiCl (50 mM)	0.45 M $LiClO_4$/DMSO	Hierarchical carbon nanocages	LiOH	Cl^-	71 cycles (500 mAh/g at 500 mA/g)	70
			Multifunctional HRMs			
InI_3 (16.7 mM)	0.5 M $LiClO_4$/DMSO	Multi-walled carbon nanotubes	Li_2O_2	In^{3+} and I_3^-	50 cycles (500 mAh/g at 500 mA/g)	75
SnI_2 (0.125 M)	1.0 M LiTFSI/DMSO + EMIM-BF_4	SnS/Reduced graphene oxide	Li_2O_2	Sn^{2+} and I_3^-	120 cycles (3000 mAh/g at 3000 mA/g)	76
$InBr_3$ (16.7 mM)	1.0 M LiTFSI/TEGDME	Multi-walled carbon nanotubes	Li_2O_2	In^{3+} and Br_3^-	206 cycles (1000 mAh/g at 250 mA/g)	77
$MgBr_2$ (25 mM)	1 M $LiClO_4$/ DMSO	Super P	Li_2O_2	Mg^{2+} and Br_3^-	120 cycles (1000 mAh/g at 500 mA/g)	78
CsI (0.05 M)	0.5 M LiTFSI + 0.5 M $LiNO_3$/ TEGDME	Carbon nanotubes	Li_2O_2	Cs^+ and I_2	130 cycles (1500 mAh/g at 500 mA/g)	79
$BrCH_2CH_2SO_3Li$ (5 wt%)	1.0 M $LiNO_3$ /DMA	Super P	Li_2O_2	$(CH_2)_2SO_3^-$ and Br_3^-	30 cycles (800 mAh/g at 0.08 mA/cm^2)	43
$BrCH_2NO_2$	Gel electrolyte	Gel-derived cathode	Li_2O_2	$CH_2NO_2^+$ and Br_3^-	120 cycles (1000 mAh/g at 500 mA/g)	80
MMP^+Br^- (0.2 M)	0.5 M LiTFSI/TEGDME	Super P	Li_2O_2	MMP^+ and Br_3^-	30 cycles (1000 mAh/g at 500 mA/g)	81
$(CH_3)_3SiBr$ (0.1 M)	1.0 M LiTFSI/DMSO	Multi-walled carbon nanotubes	Li_2O_2	$(CH_3)_3Si^+$ and Br_3^-	110 cycles (1000 mAh/g at 1000 mA/g)	82
$CF_3(CF_2)_2I$ (0.2 M)	1 M $LiNO_3$/DMA	Carbon nanotube film	Li_2O_2	$CF_3(CF_2)_2^+$ and I_3^-	100 cycles (5 mAh/cm^2 at 0.5 mA/cm^2)	83
TES^+I^- (50 mM)	Gel electrolyte	Gel-derived cathode	Li_2O_2	TES^+ and I_3^-	60 cycles (1000 mAh/g at 500 mA/g)	44
C_3H_5OI (50 mM)	1 M LiTFSI/TEGDME	Single-walled carbon nanotubes	Li_2O_2	$C_3H_5O^+$ and I_3^-	150 cycles (1000 mAh/g at 1000 mA/g)	84
			Other Functions			
LiI (0.05 M)	0.25 M LiTFSI/DME	Reduced graphene oxide-MoS_2	$Li_2MoO_2S_2$ and Li_2O_2	IO^- and I_3^-	500 cycles (500 mAh/g at 250 mA/g)	85
LiCl (0.1 M)	0.5 M LiTFSI/DEGDME with 0.05 M tetrathiafulvalene	Porous graphene	Li_2O_2	Cl^-	100 cycles (1000 mAh/g at 200 mA/g)	86

https://doi.org/10.1021/cbe.4c00025
Chem Bio Eng. 2024, 1, 737−756

Table 1. continued

HRMs	Electrolytes	Cathodes	Discharge products	Active species	Cycle performance	Ref
			Other Functions			
TCCF (2 wt%)	1 M LiTFSI/TEGDME	Super P	Li_2O_2	TCCF and Cl^-	50 cycles (1000 mAh/g at 1000 mA/g)	87

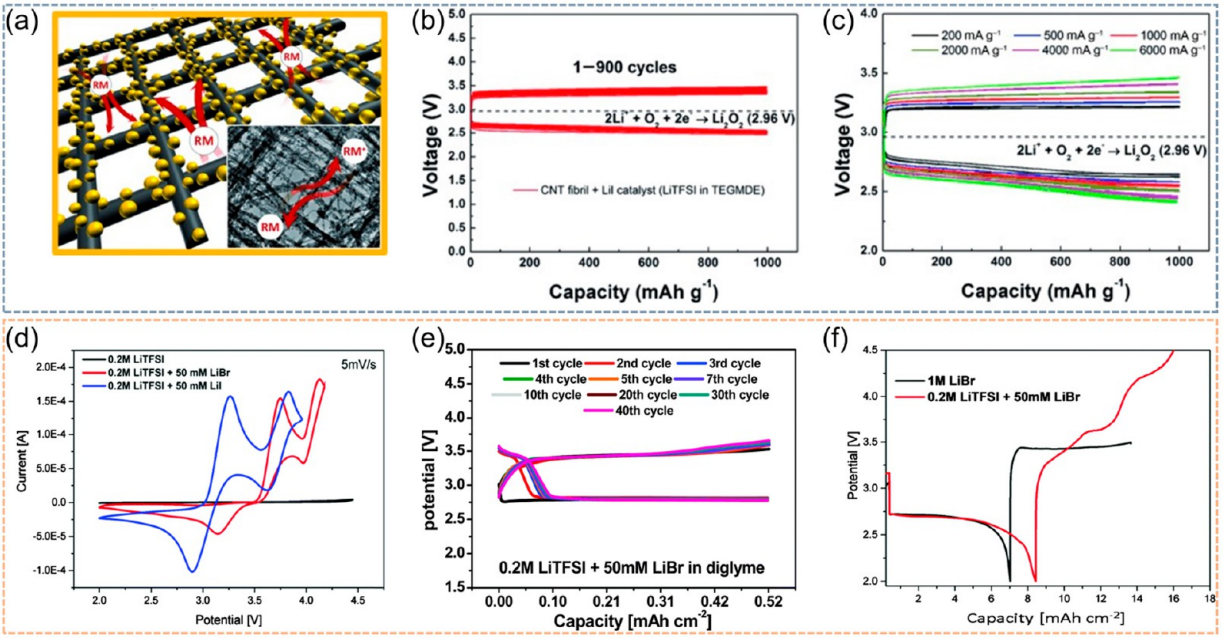

Figure 3. (a) Schematic illustration of the role of RMs in a LOB with a hierarchical CNT fibril electrode. (b) Electrochemical profiles of the CNT fibril electrode with a LiI catalyst. (c) Rate performance of the CNT fibril electrode in the presence of a LiI catalyst at current rates from 200 to 6000 mA/g. Reproduced with permission from ref 38. Copyright 2014 Wiley-VCH. (d) Cyclic voltammetry of various samples on Pt working electrodes in an Ar atmosphere. (e) Voltage profiles of LOBs during prolonged galvanostatic cycling with diglyme solutions containing 0.2 M LiTFSI plus 50 mM LiBr at a current density of 0.052 mA/cm^2. (f) Voltage profiles of LOBs containing diglyme solutions of 1 M LiBr (black curve) and 0.2 M LiTFSI plus 50 mM LiBr (red curve). Reproduced with permission from ref 37. Copyright 2016 Royal Society of Chemistry.

For halogen anions, they all possess two distinct redox couples of X^-/X_3^- and X_3^-/X_2 (X = Cl/Br/I).[27] With the increase of the charge potential, X^- is first electrochemically oxidized to X_3^- and then to X_2 on the cathode surface, as shown below (Figure 2b):[42,68]

$$3Cl^- \rightarrow Cl_3^- + 2e^- \quad E_{ethers} \approx 3.8\ V \quad (1)$$

$$2Cl_3^- \rightarrow 3Cl_2 + 2e^- \quad E_{ethers} \approx 4.2\ V \quad (2)$$

$$3Br^- \rightarrow Br_3^- + 2e^- \quad E_{ethers} \approx 3.6\ V \quad (3)$$

$$2Br_3^- \rightarrow 3Br_2 + 2e^- \quad E_{ethers} \approx 4.0\ V \quad (4)$$

$$3I^- \rightarrow I_3^- + 2e^- \quad E_{ethers} \approx 3.0\ V \quad (5)$$

$$2I_3^- \rightarrow 3I_2 + 2e^- \quad E_{ethers} \approx 3.5\ V \quad (6)$$

Subsequently, X_3^- or X_2 species diffuse to the surface of the solid discharge products to chemically decompose them.[15] As for the cations (except for Li^+), they do not take part in the decomposition of the discharge products but contribute to form functional layers to protect the Li anode and suppress the redox shuttling. Looking back on the development of the HRMs in LOBs, various halides were used, and different functions for them were discovered (as summarized in Table 1), which will be discussed in detail in the next section.

3. FUNCTIONS OF HRMs

3.1. Oxidizing Various Discharge Products. *Oxidizing Li_2O_2.* LiI was first used as an efficient RM in LOBs for charging. Lim et al. designed a LOB system with the LiI additives and a hierarchical nanoporous carbon nanotube (CNT) electrode, in which LiI could efficiently assist the decomposition of Li_2O_2 and the porous cathode provided rapid channels for both the reaction products and the soluble catalyst (Figure 3a). The overpotential during charge was decreased to 0.25 V, which can suppress the side reactions derived from the carbon corrosion and electrolyte deterioration (Figure 3b). As a result, the cyclability of the battery was dramatically improved, reaching 900 cycles without a notable change in the electrochemical profile. In addition, the battery also delivered excellent rate capability and could be operated at current density from 200 to 6000 mA/g (Figure 3c). However, the loading of the CNT was less than 0.02 mg, meaning that the actual capacity and current were tiny. A high loading of the cathode material is required for high-energy-density LOBs. Although the researchers did not look deeply into the mechanism, the excellent cell performance showed great prospects of their strategy. In order to work at ambient conditions or assemble into flexible devices, the liquid electrolyte in LOBs should be replaced with a solid or quasi-solid one. In this regard, LiI was also used in a polymer gel electrolyte or gel electrolyte, which could efficiently alleviate the Li passivation induced by the attack of air, while the I^-/I_2

https://doi.org/10.1021/cbe.4c00025
Chem Bio Eng. 2024, 1, 737−756

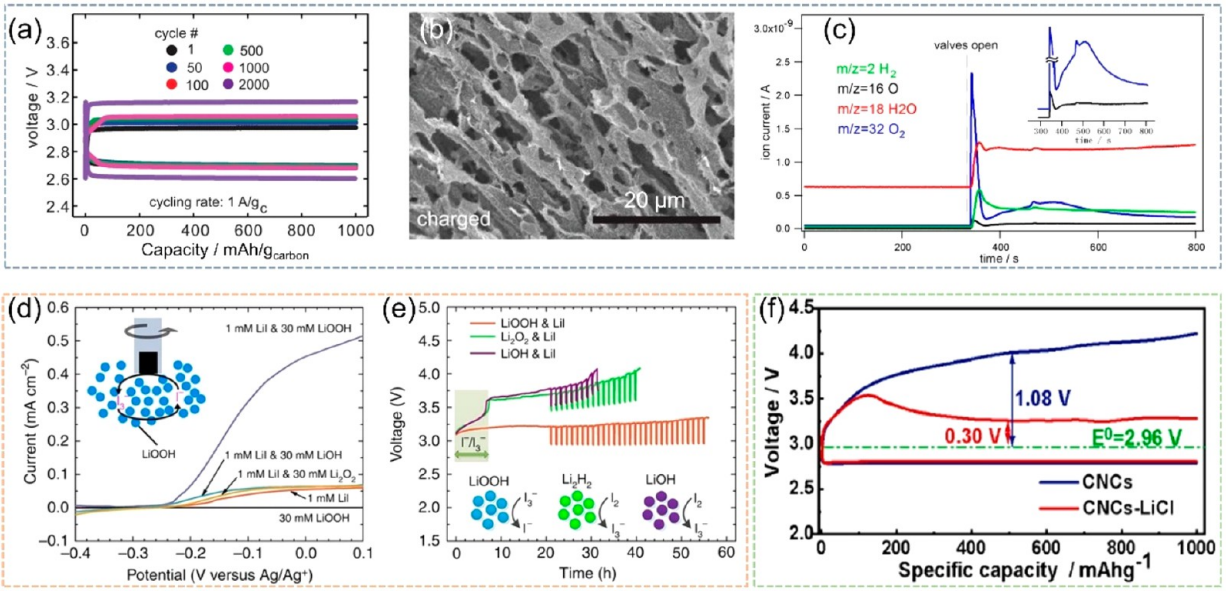

Figure 4. (a) Discharge/charge curves for LOBs using reduced graphene oxide (rGO) electrodes and a 0.05 M LiI/0.25 M LiTFSI/DME electrolyte with a capacity limit of 1000 mAh/g. (b) Image of the charged rGO electrode obtained with a 0.05 M LiI/0.25 M LiTFSI/DME electrolyte in the first cycle. (c) Mass spectrometry measurement on the gas atmosphere of the cell in (a) after it was charged under Ar. Reproduced with permission from ref 41. Copyright 2015 AAAS. (d) RDE measurements of 1 mM LiI in 0.1 M LiTFSI/DME with 30 mM LiOOH·H_2O, Li_2O_2, or LiOH dispersed in the solution. The inset illustrates the catalytic reaction between LiOOH and I_3^-. (e) Charging curves of the Li-LiOOH, Li-Li_2O_2, and Li-LiOH cells. The cells were first charged at a constant current of 0.1 mA cm^{-2} for 21 h, followed by GITT measurement (2 h charging at the same current plus 10 min resting). Reproduced with permission from ref 69. Copyright 2017 Springer Nature. (f) Discharge/charge curves of carbon nanocages (CNCs) and CNCs-LiCl cells with a fixed capacity of 1000 mAh g^{-1} (calculated based on the weight of CNCs) at a current density of 100 mA g^{-1}. Reproduced with permission from ref 70. Copyright 2020 Wiley-VCH.

conversion as a RM in the polymer electrolyte facilitated the electrochemical decomposition of the Li_2O_2-dominant discharge products during the recharge process.[67,88] Consequently, the battery can work for more than 400 cycles in air with 15% relative humidity (RH). Nevertheless, the discharge products of the above battery system tested in air were inhomogeneous, with LiOH and Li_2CO_3 as the side products, which restricted the efficacy of LiI.[67]

LiBr has a similar electrochemical behavior but exhibits higher redox potentials compared with LiI and was also used to decompose Li_2O_2 (Figure 3d). Kwak et al. found that LiBr induced fewer side reactions and was more suitable as the RM in LOBs than its LiI cousin, which was corroborated by Akella et al.[37,89] During charge, the Br^-/Br_3^- couple was competent to oxidize the Li_2O_2 discharge product at about 3.5 V, without generation of the reactive Br_2 (Figure 3e). The behavior of the Br^-/Br_3^- couple during charge was influenced by the discharge capacity, the concentration of Br^-, and the type of solvent used. A larger discharge capacity would passivate the cathode and elevate the voltage slope, which could be relieved by restricting the cut-off capacity to lower values or using a high concentration of LiBr (Figure 3f). On the other hand, diglyme as solvent, with lower viscosity and fewer contaminants, showed a more stable charge plateau than its tetraglyme counterpart. As for chloric RMs, they were rarely used to mediate the decomposition of Li_2O_2 because of their high redox potential of Cl^-/Cl_3^- (> 3.8 V), which would exhibit a poor energy efficiency. However, chloric RMs possess other advantageous features and will be discussed later.

Oxidizing LiOH. Since the discovery that LiOH can be the main discharge product by either a direct 4e$^-$ electrochemical pathway or an indirect chemical conversion pathway, considerable effort has been put forth to promote the decomposition of the insulating and redox-inert LiOH.[90] Without an effective catalyst, direct LiOH electrooxidation is difficult, as it needs a high voltage of about 4.7 V, and the first Li^+ extraction was deemed to be the rate-determining step.[91] Some solid catalysts like Ru nanoparticles were used to mediate the oxidation of LiOH, which can decrease the charge plateau to as low as 3.2 V.[92,93] However, serious side reactions, provoked by the reactive intermediates (e.g., $^{\bullet}OH$), were accompanied by the decomposition of LiOH, making the use of Ru-based materials as the catalysts questionable.[94]

As for RMs, LiI was used as a bifunctional additive in LiOH chemistry by Liu et al.[41] In their pioneering work, a battery with 0.05 M LiI showed a low charge plateau of about 3.0 V, corresponding to a potential of I^-/I_3^-, and the battery could work for more than 2000 cycles at 1 A/g (Figure 4a). After charging, the hierarchically microporous structure reappeared without the observation of flower-like LiOH deposits (Figure 4b). Significantly, a clear O_2 signal was detected by mass spectrometry in a pre-discharged battery with LiI (Figure 4c). Therefore, the researchers claimed that the charge process involves the direct electrochemical oxidation of I^- to I_3^- and the chemical oxidation of LiOH by I_3^- to generate O_2 and H_2O ($4LiOH + 2I_3^- \rightarrow 4Li + 6I^- + 2H_2O + O_2$). However, the specific mechanism of this equilibrium, which may include other I-based species, requires further investigation. Further, Zhu et al. studied the catalytic effect of I_3^- on the oxidation of LiOH as well as the other discharge products of Li_2O_2 and LiOOH in the LiI-containing battery with addition of 9.1% H_2O, by using a rotating disk electrode (RDE, Figure 4d).[69] They found that the kinetics between I_3^- and the three compounds follow the order of LiOOH > Li_2O_2 > LiOH. In the batteries preloaded with the three compounds, the battery with LiOOH presented only one prolonged charge plateau at about 3.2 V, which was determined

https://doi.org/10.1021/cbe.4c00025
Chem Bio Eng. 2024, 1, 737−756

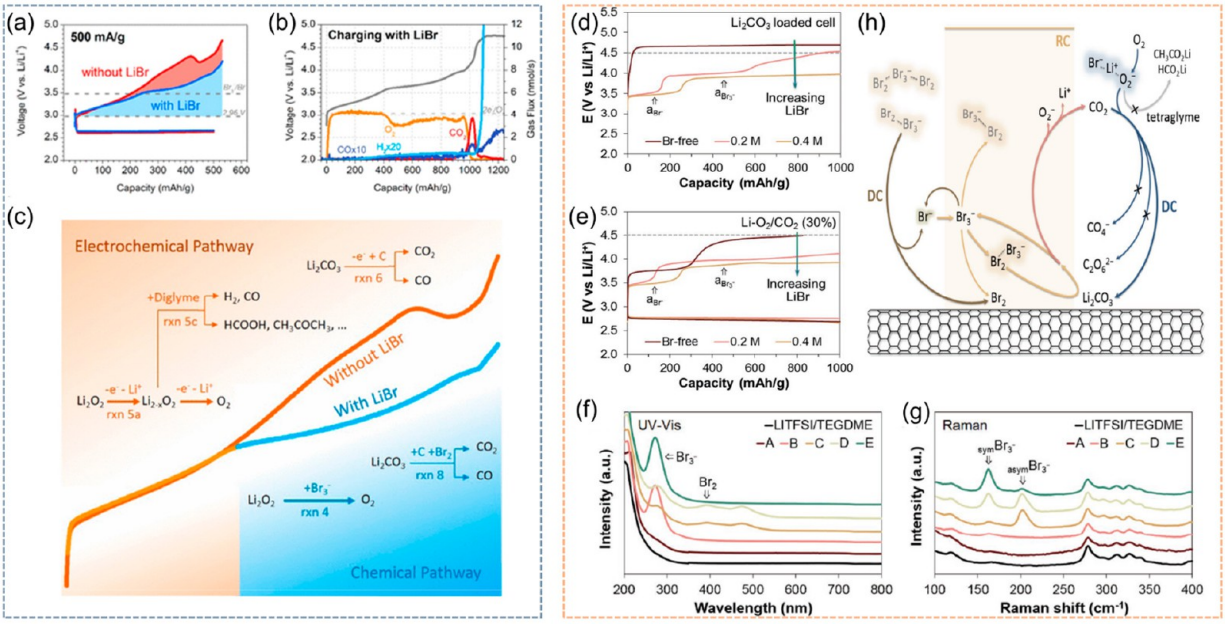

Figure 5. (a) Galvanostatic discharge/charge profiles of LOBs with and without 10 mM LiBr at 500 mA/g. (b) Voltage and gas evolution profiles during charging with 10 mM LiBr after being discharged to 1000 mAh/g at 1000 mA/g. (c) Schematic illustration of the different reaction mechanisms when charging with and without LiBr. Reproduced with permission from ref 42. Copyright 2016 American Chemical Society. (d, e) Charging process of powder Li_2CO_3 (d) and Li-O_2/CO_2 (30%) cell (e) with different concentrations of LiBr. (f, g) UV−vis absorption (f) and Raman spectra (g) at different recharge states. (h) Schematic illustration for the redox shuttling of Br_3^-/Br_2. Li_2CO_3 is formed over the CNT electrode. The Br_2···Br_3^- complex is soluble in the electrolyte solution, whereas the nonpolar Br_2 precipitates during both the discharge and recharge processes. Reproduced with permission from ref 71. Copyright 2020 Wiley-VCH.

by the I^-/I_3^- redox reaction (Figure 4e). However, for the LiOH battery, two plateaus were observed, with the plateau at about 3.7 V extended, indicating that only I_2 but not I^-/I_3^- was able to decompose LiOH, similar to the observations with the Li_2O_2 battery (Figure 4e). The Cl^-/Cl_3^- redox couple has also been used to mediate the decomposition of LiOH in a $LiClO_4$−dimethyl sulfoxide (DMSO) electrolyte with 0.05 M LiCl additive.[70] The battery with LiCl showed a low charge plateau at 3.26 V, much lower than that of the LiCl-free cell at 4.04 V (Figure 4f). However, information about O_2 evolution during charging was not given. By parity of reasoning, Br^-/Br_3^- and Br_3^-/Br_2 should also be able to facilitate the decomposition of LiOH.

Oxidizing Li_2CO_3. Li_2CO_3 was deemed as an undesirable parasite product in typical LOBs. It is typically generated from the decomposition of organic electrolyte, oxidization of the carbon-based cathode, and contamination with shuttled CO_2 gas. On the other hand, Li_2CO_3 can be the major product in CO_2-involved LOBs, a new energy storage system that could promote the conversion and utilization of CO_2.[95] However, owing to the insulation and the high thermodynamic equilibrium potential, the decomposition of Li_2CO_3 is sluggish and occurs at higher charging voltage. Ling et al. predicted that the decomposition of Li_2CO_3 requires a voltage in the range of 4.38−4.61 V via a first-principles study because it requires higher energy to oxidize the redox-inert anions when Li is extracted.[91] Undoubtedly, high charge voltages would accelerate the electrode oxidation and electrolyte decomposition, leading to the additional accumulation of Li_2CO_3 and further the early death of the battery.

As mentioned earlier, LiBr undergoes the oxidation steps of Br^-/Br_3^- (3.5 V) and Br_3^-/Br_2 (4.0 V), and the potential of the latter is slightly above the decomposition potential of Li_2CO_3 (3.82 V). Therefore, LiBr is able to mediate the oxidation of Li_2CO_3 with the assistance of the Br_3^-/Br_2 couple. Liang et al. observed that CO_2 began to evolve, accompanied by an increase in CO evolution, at about 3.9 V in the presence of LiBr from the online electrochemical mass spectra, which was much earlier than it occurred in the LiBr-free cells (4.35 V), indicating that the oxidation of Li_2CO_3 was mediated by the LiBr mediator as follows: $9Br_2 + 3Li_2CO_3 + 2C \rightarrow 6Br_3^- + 6Li^+ + 4CO_2 + CO$ (Figure 5a,b).[42] However, the mechanism of the LiBr-mediated decomposition of Li_2CO_3 is complex (Figure 5c), calling for further characterizations. Later, Mota et al. revealed the role of the Br_3^-/Br_2 redox couple in CO_2-assisted LOBs, where the film-like amorphous Li_2CO_3 was the main discharge product.[71] First, the charge voltage of the Li-O_2/CO_2 battery was lower than that of the cell loaded with commercial Li_2CO_3 powder, suggesting that the redox shuttle of Br_3^-/Br_2 decomposed amorphous Li_2CO_3 more efficiently than its crystalline counterpart, which was ascribed to the faster charge transport and higher accessible surface area of the Li_2CO_3 discharge product (Figure 5d,e). It is surprising that the Br_3^-/Br_2 redox couple could have such a high redox efficiency during the first cycle recharge, considering that the nonpolar Br_2 should be mostly precipitated before approaching Li_2CO_3. Ultraviolet−visible (UV-vis) absorption and Raman spectra were used to monitor the electrolyte at different states of charge (SOCs). The red-shifted UV-vis absorption band at 474 nm and the appearance of an antisymmetric Br_3^- stretching mode (asym-Br_3^-) pronounced at 201 cm^{-1} in the Raman spectra indicated the emergence of a Br_2···Br_3^- complex at 50% SOC (Figure 5f,g). This complex could work as a mobile catalyst so that the Br_2 could access and decompose Li_2CO_3 without precipitation (Figure 5h). However, the precipitation of Br_2 on the CNT electrode still

https://doi.org/10.1021/cbe.4c00025
Chem Bio Eng. 2024, 1, 737−756

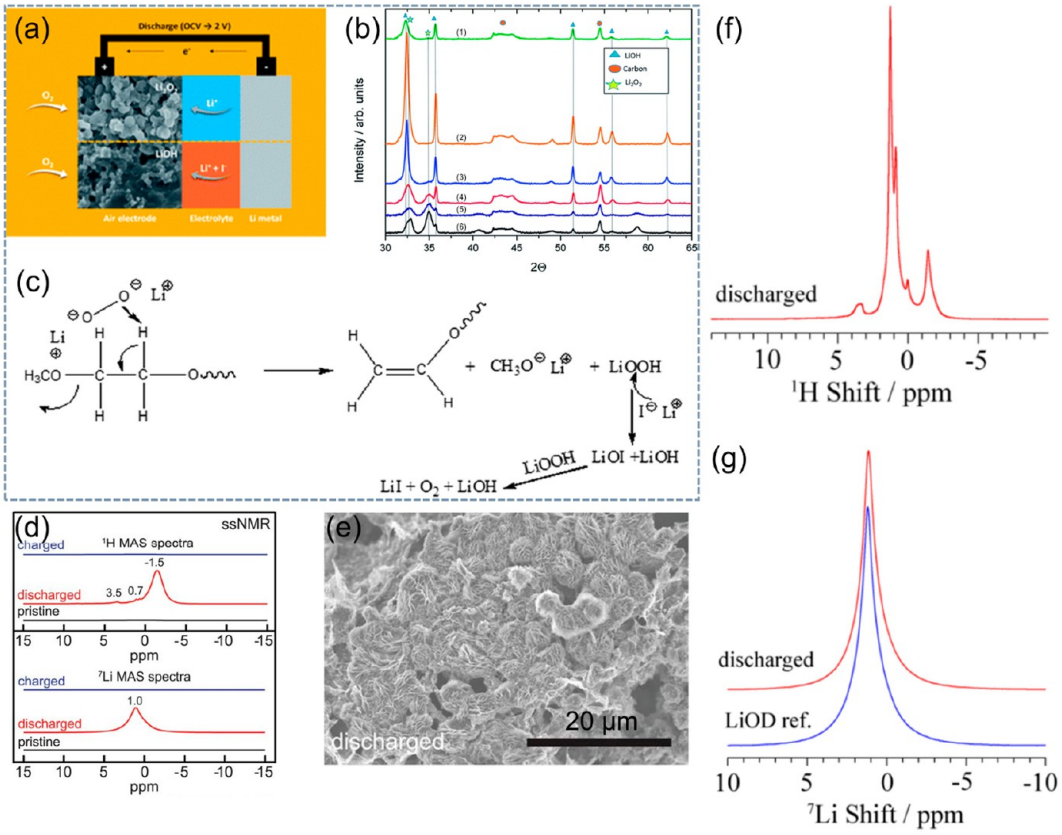

Figure 6. (a) Schematic diagram showing that the discharge products convert from Li_2O_2 to LiOH when LiI additives are introduced. (b) XRD patterns of the gas diffusion layer (GDL) electrode discharged to 2 V using TEGDME with (1) 1 M LiI; (2) 1 M LiTFSI + 100 mM LiI; (3) 1 M LiTFSI + 10 mM LiI; (4) 1 M LiTFSI + 10 mM LiI stopped at 2.6 V; (5) 1 M LiTFSI + 5 mM LiI; and (6) 1 M LiTFSI. (c) Proposed decomposition reaction mechanism of ether solvents in LOBs containing LiI. Reproduced with permission from ref 72. Copyright 2015 Royal Society of Chemistry. (d) ^{1}H and ^{7}Li ssNMR spectra comparing a pristine rGO electrode to electrodes at the end of discharge and charge in a 0.05 M LiI/0.25 M LiTFSI/DME electrolyte. (e) Image of a fully discharged rGO electrode obtained with a 0.05 M LiI/0.25 M LiTFSI/DME electrolyte in the first cycle. (f, g) ^{1}H (f) and ^{7}Li (g) ssNMR spectra of the rGO electrodes prepared using a 0.05 LiI/0.25 M LiTFSI/non-deuterated DME electrolyte but with added D_2O (20,000 ppm, 15 mg). Reproduced with permission from ref 41. Copyright 2015 AAAS.

happened at the end of the recharging and was harmful to the cycling of the batteries.

3.2. Mediating the Generation of LiOH. In the nascent stage of LOBs, LiOH was taken as the side product and eliminated as much as possible to reduce the cumulative negative impact. For example, polyvinylidene binder was susceptible to superoxide intermediates and dehydrofluorinated to give a byproduct of LiOH.[18] In another case, flake-like LiOH gradually extended along Li_2O_2 particles exposed to DMSO-based electrolyte, caused by the chemical reaction of electrolyte with Li_2O_2 and superoxide species.[96] Thereafter, Kwak et al. found that LiOH rather than Li_2O_2 became the main discharge product in tetraethylene glycol dimethyl ether (TEGDME) solution with 1 M LiI, as confirmed by X-ray diffraction (XRD) and scanning electron microscopy (SEM) results (Figure 6a,b).[72] They argued that I^- promoted the fast decomposition of LiOOH, which was formed by the E2 elimination between lithium peroxide or superoxide and TEGDME, to generate LiOH and LiOI. The latter reacts in turn with additional LiOOH, leading to the formation of O_2, LiI, and more LiOH (Figure 6c). When the concentration of I^- was low (e.g., 0.1 M), the competing side reaction causing the production of LiOH was sluggish and Li_2O_2 became the main product (Figure 6b). Qiao et al. verified that LiI could promote the nucleophilic reactions between the discharge intermediates and the electrolyte molecules.[73] As Kwak et al. suggested, the proton of LiOH was mainly from the solvent molecules, meaning that the generation of LiOH was accompanied by side reactions, and thus iodide was not considered to be a satisfactory additive.

Soon after, Grey's group added H_2O and LiI to the DME-based electrolyte, and they found that the discharge product was overwhelmingly LiOH, even at a low concentration of LiI (0.05 M) (Figure 6d).[41] The LiOH showed a flower-like morphology tens of microns in size, indicating a solution growth pathway (Figure 6e). In addition, the researchers claimed that LiOH formation occurred through a stoichiometric $4e^-$ ORR ($4Li^+ + 2H_2O + O_2 + 4e^- \rightarrow 4LiOH$), in which H_2O was the main proton source and both H_2O and O_2 served as the O sources, as evidenced by solid-state NMR with isotopic labeling (Figure 6f,g). As for the detailed mechanism, they suggested that the first step on discharge was an electrochemical reaction where O_2 was reduced to form LiO_2, followed by a chemical process of LiO_2 converting into LiOH with the assistance of I^-. McCloskey et al. and Tułodziecki et al. also showed that LiOH was the main discharge product in the H_2O and LiI co-presenting systems, while LiI or H_2O alone cannot mediate the formation of LiOH,[68,74] which was inconsistent to the results of Kwak et al. and Qiao et al. discussed above. It should be noted that the battery system with both H_2O and LiI was much more stable because the DME decomposition caused by the reactive

https://doi.org/10.1021/cbe.4c00025
Chem Bio Eng. 2024, 1, 737−756

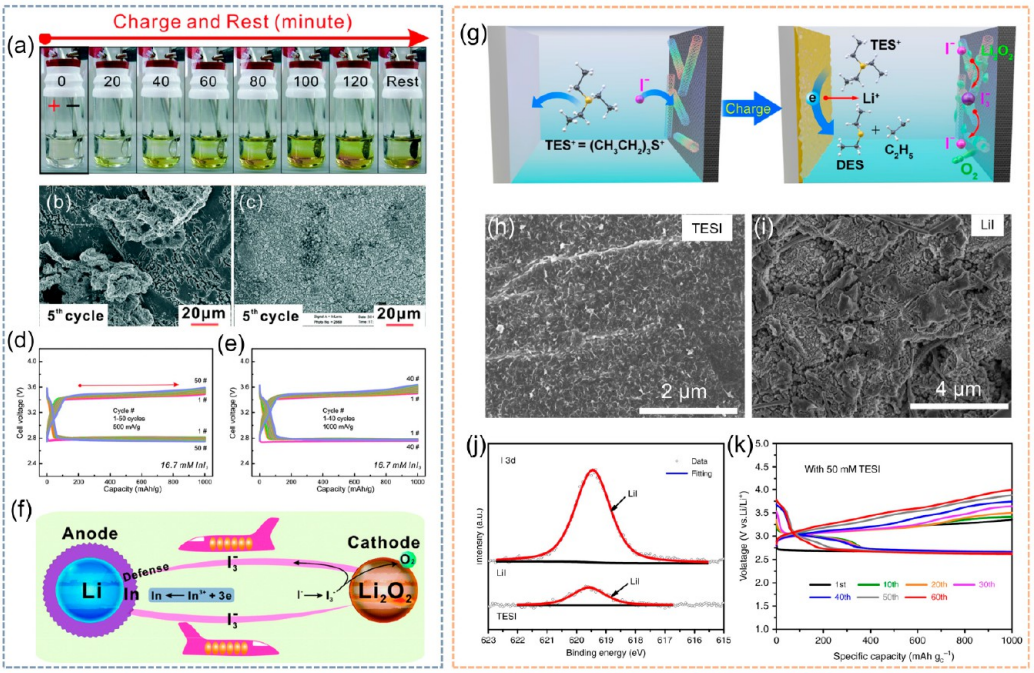

Figure 7. (a) Visual observation of the Li-O_2 beaker cell recorded as charging proceeds. (b, c) Comparison of the micrograph images of the Li surface in the LiI-containing (b) and the InI_3-containing LOB (c) after the fifth cycle at 500 mA/g. (d, e) Cycling performance of the LOBs with the DMSO-based electrolyte containing 16.7 mM InI_3 at 500 mA/g (d) and 1000 mA/g (e). (f) Working mechanism for a self-defense RM of InI_3. Reproduced with permission from ref 75. Copyright 2016 Royal Society of Chemistry. (g) Schematic illustration of the *in situ* formation process of the SEI-like layer on the Li anode during charging. (h, i) SEM images of the Li anode after 60 cycles with 50 mM TESI (h) and after 30 cycles with 50 mM LiI (i). (j) I 3d spectra on the surface of Li anodes. (k) Electrochemical performance of the LOB with 50 mM TESI at 500 mA/g. Reproduced with permission from ref 44. Copyright 2019 Springer Nature.

intermediate (LiO_2) could be substantially reduced and the mild LiOH appeared to cause minimal chemical reactions with the electrolyte and the carbon cathode compared to the Li_2O_2 counterpart. Other than LiOH, $LiOOH{\cdot}H_2O$ was also detected after discharge in the H_2O-containing LOBs with LiI additives. This new lithium compound showed a distinct physicochemical property compared with LiOH and could be a promising discharge product for high-performance LOBs.[97] Overall, the introduction of both LiI additives and proton sources into LOBs would convert the Li_2O_2 chemistry into the LiOH chemistry. Nevertheless, the chemistry with Li^+, O_2, H_2O, and LiI is quite complex, which will be further discussed later.

Besides LiI, LiCl was also reported as a promoter for LiOH chemistry in the DMSO-based electrolyte, but the relevant mechanism was not given, only with the suggestion that a residual H_2O or DMSO molecule was the proton source.[70] Surprisingly, among the three LiX additives, only LiBr was found not to induce the generation of LiOH. The different behaviors of various halide additives during discharge and the mechanism for the formation of LiOH mediated by the halide species require further study. It is worth mentioning that some special solid catalysts (e.g., Co_3O_4 and CoN_3-G) and cation additives (e.g., Na^+) can also mediate the generation of LiOH during discharging.[98−100]

3.3. Multifunctional HRMs. Typical LOBs are not only plagued by the problems associated with cathode (e.g., the difficult removal of discharge products and the germination of the side reactions under high charge potential) but also suffer from issues related to the Li anode (e.g., dendrite growth, instability in the electrolyte, and the $O_2/CO_2/H_2O$ and RM crossover).[14] As it is known that LiX additives with various active couples can relieve the cathode issues to a large extent, some artificial SEI or SEI-formed additives were used to protect the Li anode.[101] Finding an additive that is able to address the issues confronted in both cathode and anode to simplify the battery system is intriguing.

A class of RMs, named as self-defense RMs, with the formula of MX (M denotes certain metals), have been developed as multifunctional additives in LOBs. Zhang et al. observed a shuttle phenomenon in a visual beaker cell with LiI in DMSO as the electrolyte, in which the oxidizing I_3^- would diffuse to the Li anode and be reduced to LiI (Figure 7a). When LiI was replaced with InI_3, the battery could suppress the growth of dendrites (Figure 7b,c) and showed stable cycle life and rate performance (Figure 7d,e). It was found that In^{3+} would deposit on the surface of the Li anode and form a thin indium layer, which could resist attack by I_3^- as the reaction between indium and iodine is sluggish (Figure 7f). However, forming an Li-In alloy and the presence of even marginal lithium during cycling would destroy the protective indium layer. Besides InI_3, other metal iodides/bromides, including SnI_2,[76] $InBr_3$,[77,102] and $MgBr_2$,[78] were also employed as multifunctional RMs. On the other hand, some alkali metal ions (e.g., Rb^+ and Cs^+), which remained as cations even after the deposition of Li at low concentrations, could serve as an "electrostatic shield" at the sharp points of the Li anode to hinder the further reduction of Li^+ at those points. Lee et al. used CsI as a multifunctional additive in a LOB, which showed better battery performance manifested by the reduced overpotential and the suppressed growth of Li dendrites.[79]

As mentioned above, the use of an inorganic metallic protective layer (e.g., indium metal layer) could not protect the Li anode very well because it is an electronic conductor. The

https://doi.org/10.1021/cbe.4c00025
Chem Bio Eng. 2024, 1, 737−756

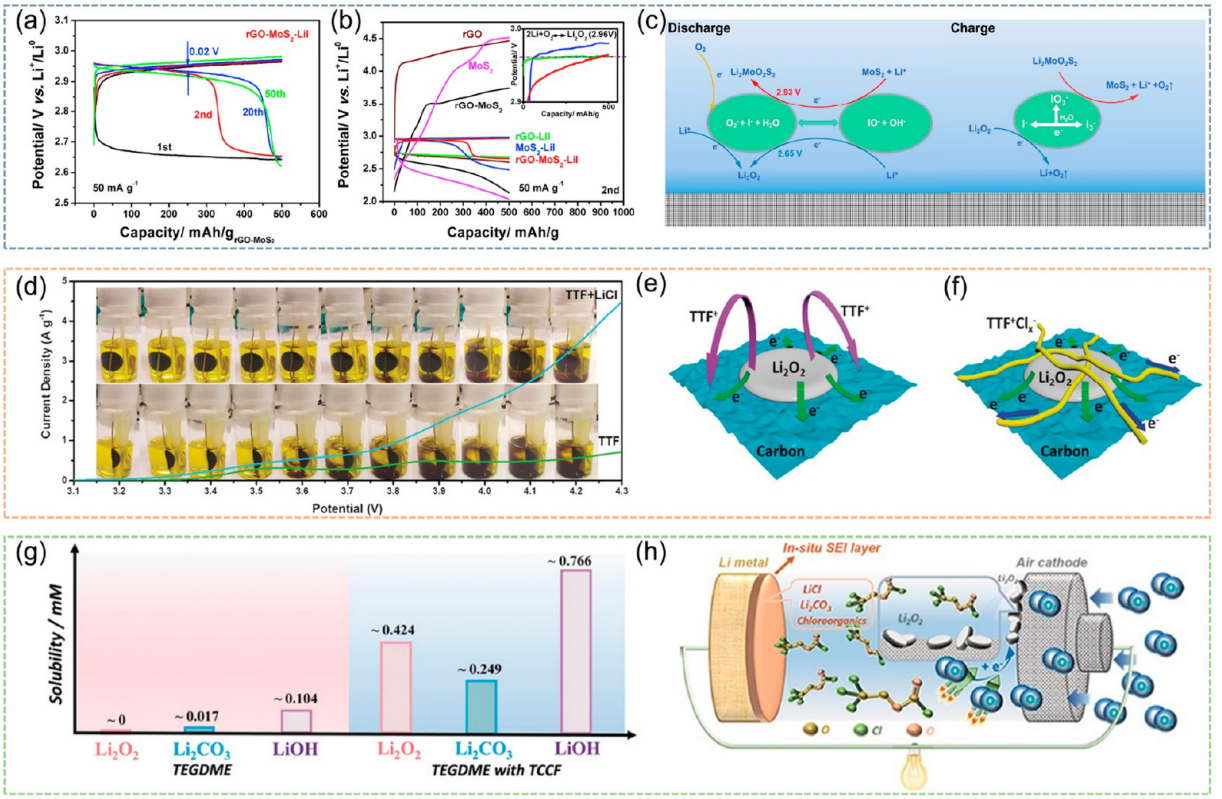

Figure 8. (a) Selected potential curves of the rGO-MoS_2 with LiI at different cycles. (b) Comparison of the potential curves of rGO, MoS_2, and rGO-MoS_2 with and without LiI at the second cycle. (c) Schematic of the reaction mechanism of rGO-MoS_2 with LiI during discharge and charge. Reproduced with permission from ref 85. Copyright 2018 Elsevier. (d) Digital photos of a two-electrode device with the TTF electrolyte and TTF + LiCl electrolyte. Superimposed are plots of current density versus potential for TTF^+Cl^- (blue) and TTF (green). (e, f) Schematic illustration of the mechanism of $TTF^+Cl_x^-$ facilitating the decomposition of Li_2O_2. Reproduced with permission from ref 86. Copyright 2017 Wiley-VCH. (g) Saturation concentrations of Li_2O_2, LiOH, and Li_2CO_3 in a TEGDME solvent with/without TCCF. (h) Schematic illustration of the mechanism of TCCF boosting the rate capability and contributing to a LiCl-rich SEI. Reproduced with permission from ref 87. Copyright 2019 Wiley-VCH.

employment of an organic film to replace the metal one is a favorable choice. Several organo-halogen compounds, like bromide ionomers,[43] bromonitromethane,[80] *N*-methyl-*N*-propylpyrrolidine bromide,[81] imidazolium bromide,[103] triethylsulfonium iodide,[44] and fluoroalkyl iodide,[83] have been developed recently as multifunctional additives for LOBs. Choudhury et al. deliberately selected an ionomer salt additive, called 2-bromoethanesulfonate lithium salt, that reacted with Li metal to simultaneously form a lithium ethanesulfonate-based SEI and liberate partially soluble LiBr into the electrolyte.[43] The *in situ* generated SEI (about 15 nm) could not only enable the stable and fast Li deposition but also protect the Li anode from chemical attack by a high donor number (DN) electrolyte. Additionally, the partially soluble LiBr acted as a RM to improve the energy efficiency of the battery. In another work, Zhang et al. chose a triethylsulfonium iodide (TESI) additive among various organic iodide since TES^+ could be easily reduced by lithium and then oxidized by O_2/O_2^-, generating an organic-dominant film (Figure 7g).[44] The as-formed insulating SEI-like layer coated on the surface of Li anode could restrict the growth of dendrites and the shuttling of RMs, as evidenced by comparing the morphology of the Li anode (Figure 7h,i) and the LiI content on the Li surface with those of the LiI-containing battery (Figure 7j). With the help of the robust organic and inorganic composite interface, the LOB with 50 mM TESI exhibited excellent stability over 60 cycles with relatively small overpotential as well as stable discharge plateaus (Figure 7k). As suggested, the functions of the *in situ* formed SEI-like film are determined by the chemical structure of the organic cation, so we could resort to theoretical calculations for selecting a suitable cation to obtain a desirable protective layer.

3.4. Other Unique Functions. Besides the above functions, some special effects of HRMs have been discovered, like mediating and decomposing new discharge product (i.e., $Li_2MoO_2S_2$), enhancing the conductivity of Li_2O_2 discharge product, increasing the solubility of Li_2O_2, and so on. Wang et al. developed a new hybrid Li-ion/Li-O_2 battery consisting of a reduced graphene oxide (rGO)-MoS_2 cathode, LiI mediator with $Li_2MoO_2S_2$, and Li_2O_2 as the discharge products.[85] The galvanostatic discharge/charge curves of the battery showed a lower discharge plateau (the formation of the O_2^-/IO^- radicals) at the first cycle, a higher plateau (the oxidation of MoS_2 through oxyhalogen−sulfur electrochemical reactions) at the following cycles, and a charge plateau less than 3 V (the electrochemical oxidation of I^-), contributing to the superior energy efficiency approaching 99% (Figure 8a). Significantly, it was the synergistic effect between LiI and MoS_2 that led to the $Li_2MoO_2S_2$ pathway (Figure 8b). Detailed mechanism studies revealed that the IO^- species, which were generated through the reaction between superoxide, LiI, and trace H_2O, were the mediators for the formation of $Li_2MoO_2S_2$ during discharge, while the I_3^- and IO^-/IO_3^- that emerged during charge were believed to facilitate the decomposition of $Li_2MoO_2S_2$ and Li_2O_2 (Figure 8c).

https://doi.org/10.1021/cbe.4c00025
Chem Bio Eng. 2024, 1, 737−756

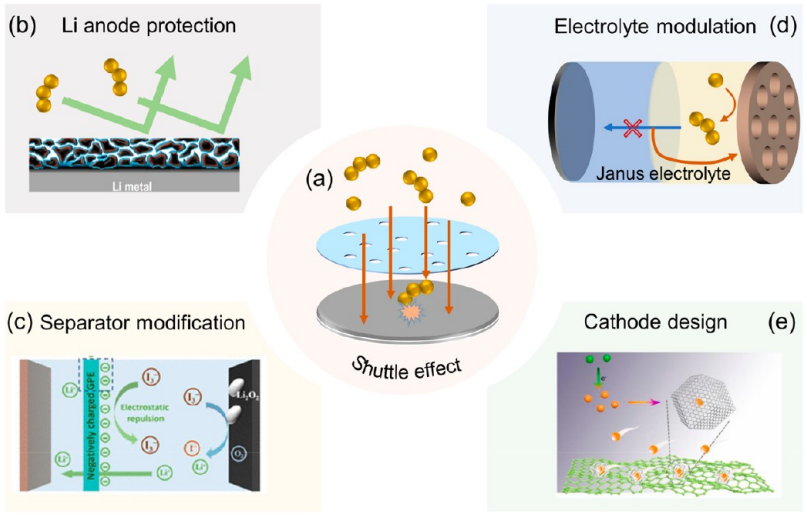

Figure 9. (a) Illustration of the shuttling of HRMs. (b) Protecting the Li anode to suppress the reaction between oxidizing HRMs and Li metal. (c) Modification of the separator to limit the transportation of oxidizing HRMs to the anode. Reproduced with permission from ref 107. Copyright 2021 American Chemical Society. (d) Modulating the electrolyte to confine HRMs in the catholyte side. (e) Designing the cathode to capture oxidizing HRMs. Reproduced with permission from ref 110. Copyright 2021 Elsevier.

Nevertheless, the energy density of $Li_2MoO_2S_2$-based batteries is quite low compared to that of Li_2O_2-based LOBs.

Cl-based RMs were seldom used to oxidize the discharge products or side products because of the high redox potentials of Cl^-/Cl_3^- or Cl_3^-/Cl_2, but their other effects enabled the high performance of LOBs. Zhang et al. discovered that Cl^- could coordinate with a tetrathiafulvalene cation (TTF^+) to form a solid compound, $TTF^+Cl_x^-$, that precipitated on the cathode and separator, which decreased the shuttling of TTF and alleviated the associated side reactions (Figure 8d). In addition, compared to the bare Li_2O_2 on the carbon support, the electronically conductive $TTF^+Cl_x^-$ provided a faster solid–solid pathway for electron transfer, which was beneficial for the decomposition of the discharge products (Figure 8e,f). This study provides us a new direction to restrict the migration of organic RMs to improve the battery performance, but further work, like modification of the diaphragm and the cathode, is needed to relieve the cumulative loss of TTF on the separator. In another case, Wang et al. employed a halide ester, 2,2,2-trichloroethyl chloroformate (TCCF), as a versatile additive. The ether-based electrolyte with TCCF exhibited enhanced solubility of Li_2O_2 and improved migration of O_2 across the electrode–electrolyte interface, leading to the superior rate performance (Figure 8g,h). In addition, the *in situ* formed LiCl-rich SEI formed by the reaction between Li and TCCF facilitated the stable Li stripping and deposition (Figure 8h), making a safe and stable Li anode. The LiCl-rich SEI was also achieved by using $SOCl_2$ additives.[104] However, the higher solubility of Li_2O_2 may induce the more serious side reactions because of the larger contact area between Li_2O_2 and electrolyte. Besides, Cl^- can also be incorporated into the Li_2O_2 films during discharge to increase the discharge capacity.[105]

4. CHALLENGES AND CONTROVERSIES

As mentioned above, HRMs possess various functions for boosting the performance of LOBs. However, some inherent shortcomings of these HRMs as well as several ambiguous aspects present in the discharge/charge processes hinder their further developments. These challenges, solving strategies, and the main controversies will now be discussed.

4.1. Shuttle Effect. Due to the solubility of the HRMs, the oxidizing RM species generated on the cathode can shuttle to the anode freely (Figure 9a). The oxidizing RMs at the anode would be reduced by the Li, inducing the self-discharge and the decrease of the Li_2O_2 decomposition efficiency.[27] The shuttle effect would also deteriorate the Li anode and deplete the RMs, leading to the shortened cycle life of the battery.[21] In addition, for some organic halide compounds, side products derived from the decomposition of the organic cations, would shuttle back to the cathode and poison it.[21] In order to restrict the shuttling of RMs, some strategies for modifying the Li anode, separator, cathode, and electrolyte have been proposed.

First, some artificial protective films on the anode, like a graphene–polydopamine coating layer and iodine-containing polymer/alloy layer and various *in situ* formed SEI-like interfacial layers, as mentioned in section 3.3, were well designed to forbid the physical contact between Li and RM species.[43,44,106] The protective layers are required to have sufficient ionic conductivity but low electronic conductivity, good stiffness, and high chemical stability. For example, Kwak et al. designed a graphene–polydopamine coating layer that inherited the mechanical flexibility of graphene and the adhesion properties of polydopamine.[106] This advanced composite coating layer suppressed the dendrite growth and prevented side reactions of RM, H_2O, and O_2 with the Li anode (Figure 9b). As a result, the battery with the coated anode showed extended cycle life (>150 cycles) compared to the counterpart with the bare Li anode (~16 cycles). Modifying the separator is also a promising method to imprison the RM species on the cathode side. For example, the negatively charged groups/materials (e.g., $-SO_3-$ and Nafion) grafted on the separator could confine the oxidizing halide species (e.g., Br_3^- and I_3^-) by electrostatic repulsion force (Figure 9c).[107] Similarly, simply replacing the negatively charged group/material with positively charged ones enabled the confinement of the cation-type RMs. On the other hand, adjusting the pore size of the separator to allow the permeation of Li^+ but not the RMs would also suppress the shuttling, but it was difficult to realize because of the similar ionic radii of Li^+ and Br_3^-/I_3^-.[108] As for regulating the electrolyte, some researchers introduced solid electrolytes

https://doi.org/10.1021/cbe.4c00025
Chem Bio Eng. 2024, 1, 737–756

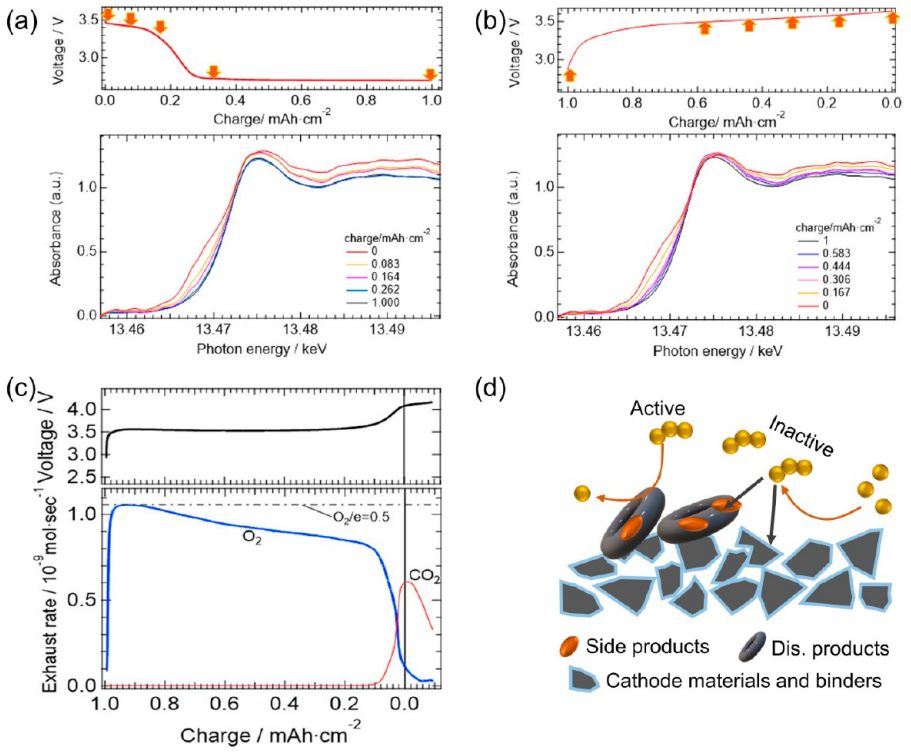

Figure 10. (a, b) Voltage profiles of the second discharge (a) and the first recharge (b) (upper panels). Br K-edge XANS spectra obtained at the points indicated by the arrows are shown in the lower panels. (c) Voltage profile and DEMS profiles of O_2 and CO_2 during the first recharge. Reproduced with permission from ref 112. Copyright 2022 American Chemical Society. (d) Possible mechanism for the inactivity of HRMs.

(e.g., sodium superionic conductor) to prevent redox shuttling, but the ionic conductivity of the solid electrolytes is usually inferior to that of the liquid ones.[73] Ko et al. designed an all-liquid-based hybrid electrolyte, also named a liquid-based Janus electrolyte, which was made up of catholyte (1 M lithium bis(trifluoromethanesulfonyl)imide (LiTFSI) in DMSO) and anolyte (2.3 M LiTFSI in TEGDME).[109] The Janus electrolyte was realized by adjusting the lithium salt concentrations in the solvents to maximize the discrepancy in the solubility parameters between the catholyte and anolyte. Significantly, the TEGDME in the anolyte was compatible with the Li anode, and DMSO in the catholyte was relatively stable for the oxygen electrochemistry. In addition, the RM species (i.e., I_3^-) would be confined in the catholyte because DMSO with higher permittivity exhibits stronger solvation of I_3^- than TEGDME (Figure 9d). Consequently, the battery with the liquid-based Janus electrolyte showed a much prolonged cycle life. Constructing a cathode material with a porous structure and/or decorated with polar species could also hinder the redox shuttling. For example, ZnO-decorated/nitrogen-doped carbon cages on rGO captured Br_3^- by space confinement effects and/or chemisorption (Figure 9e).[110] Additionally, the strong binding between RuO_2 and I_2 as well as the solvation effect of DMSO on I_2 synergistically suppressed the shuttling effect of I species.[111] It is believed that it is impossible to entirely solve the shuttling issue of RM species by one single strategy for achieving a long cycle life of LOBs, but combining two or more of the methods listed above might be more desirable.

4.2. Inactivity of the Oxidizing HRMs. As it can be noticed from the reported works that the shape of the discharge curve changed after the first cycle. Taking LiBr-mediated LOBs as an example, a high plateau appeared before the low plateau associated with the reduction of O_2 at the second discharge curve (Figure 10a). Ito et al. studied the (electro)chemical behaviors of Br^-/Br_3^- by *operando* Br K-edge dispersive X-ray absorption fine structure (XANS).[112] During the first cycle, the concentration of Br_3^- increased monotonically after ~30% charging, indicating that partial Br_3^- formed via the oxidation of Br^- did not oxidize Li_2O_2 as RM but accumulated in the cell (Figure 10b). Consequently, a higher discharge plateau, assigned to the reduction of Br_3^-, was present, and it contributed to ~20% of the total discharge capacity, which was consistent with the 83% O_2 restoration during charge (Figure 10c). It remained an open question why the partial Br_3^- is inactive. The authors believed that some Br_3^- was adsorbed on the surface of the byproducts (e.g., Li_2CO_3), which could not be decomposed by Br_3^- (Figure 10d). Other components like the binder might also deactivate the RMs. If so, using a more stable electrolyte and cathode to reduce the generation of byproducts and employing a self-supporting electrode without binder might enhance the faradaic efficiency of HRMs.

4.3. Controversies during Discharge. Since the discovery that LiI additives could transfer Li_2O_2 chemistry into LiOH chemistry in LOBs, much attention was focused on uncovering the discharge mechanism. However, the battery systems containing Li^+, O_2, I^-, solvent molecules, and even H_2O were extremely complex. The main open questions/controversies in this field are as follow: (1) Is H_2O or a solvent molecule the dominant proton source for the formation of LiOH (Figure 11a)? (2) What is the true species that triggers the solvent/H_2O deprotonation (Figure 11a)? (3) What is the LiOH formation mechanism mediated by the I-based species (Figure 11b)? (4) Why were miscellaneous discharge products generated in the electrolyte with high H_2O content (Figure 11c)?

https://doi.org/10.1021/cbe.4c00025
Chem Bio Eng. 2024, 1, 737−756

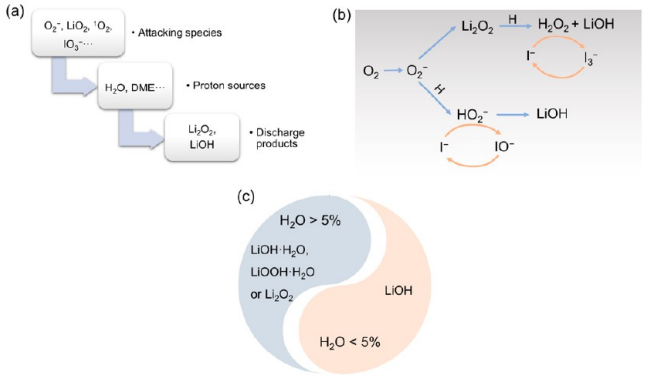

Figure 11. (a) Disputations on the proton sources and attacking species in LiOH-based LOBs containing LiI additives. (b) Possible LiOH formation mechanism mediated by the I-based species. (c) Conversion of discharge products from LiOH to others with the increased H_2O content.

Is H_2O or a solvent molecule the dominant proton source for the formation of LiOH? Kwak et al. and Qiao et al. found that LiOH and other carboxylates were formed in nominally dry batteries with LiI additives (especially with high concentration of LiI, Figure 12a).[72,73] Therefore, they claimed that the ether-based solvent, the only available proton source in the system, was responsible for the production of LiOH, corroborated by the generation of carboxylates from the decomposition of the solvent. On the other side, Burke et al. found that the LiI additives alone in the batteries formed Li_2O_2 rather than LiOH, while LiOH was formed in the co-presence of H_2O and LiI.[68] In addition, the isotopic labeling experiments showed that LiOD was formed only when both LiI and D_2O were added into the electrolyte, indicating the H in LiOH came from H_2O instead of the DME solvent. Furthermore, Tułodziecki et al. observed that both ether-based solvent and H_2O could be deprotonated for producing LiOH at the low-H_2O-content condition.[74] Whether a solvent is the dominant proton source might be dependent on its own deprotonation energy, which needs further support from theoretical calculations.[113] One can also decide whether a solvent can be the dominant proton source by quantifying the discharge products in a battery with lean anhydrous LiI-including electrolyte under a large discharge capacity. If the amounts of LiOH are comparable to the amounts of solvent, the solvent would be the main proton source; the solvent would otherwise not be the dominant proton provider. It is worth

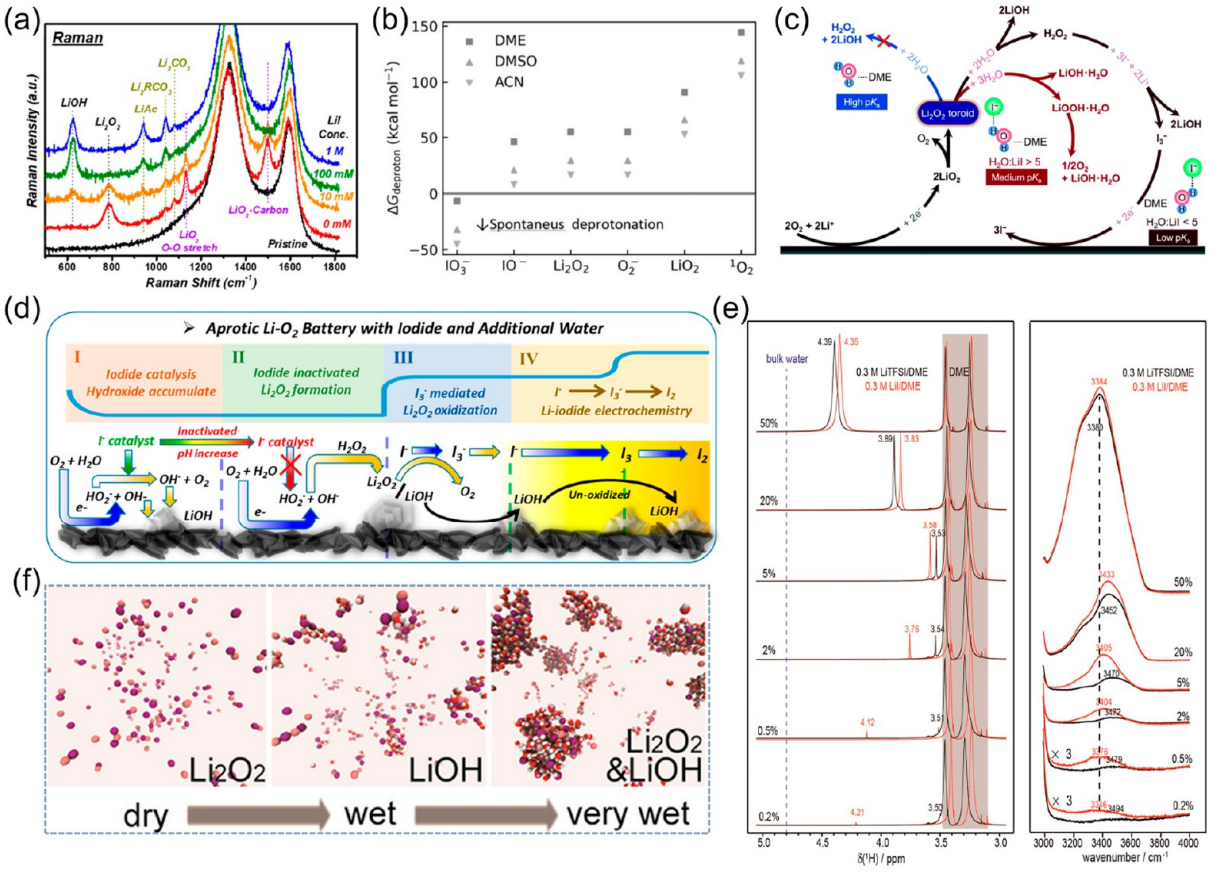

Figure 12. (a) Raman spectra of the discharge products in LOBs with varying LiI contents. Reproduced with permission from ref 73. Copyright 2017 American Chemical Society. (b) Predicted effect of nucleophiles on the deprotonation of common solvents. Reproduced with permission from ref 115. Copyright 2023 Wiley-VCH. (c) Schematic of the discharge process in the presence of H_2O and LiI in DME-based electrolyte. Reproduced with permission from ref 74. Copyright 2017 Royal Society of Chemistry. (d) Proposed reaction mechanism in iodide-containing LOB systems with some H_2O. Reproduced with permission from ref 73. Copyright 2017 American Chemical Society. (e) Analysis of the electrolyte (containing different ratios of LiI and H_2O) by ^1H solution NMR (left) and FT-IR (right) spectroscopies. (f) Molecular dynamics simulation snapshots, showing Li^+, I^-, and H_2O, of the LiI/DME electrolyte as a function of increasing H_2O content. Reproduced with permission from ref 118. Copyright 2018 American Chemical Society.

https://doi.org/10.1021/cbe.4c00025
Chem Bio Eng. 2024, 1, 737−756

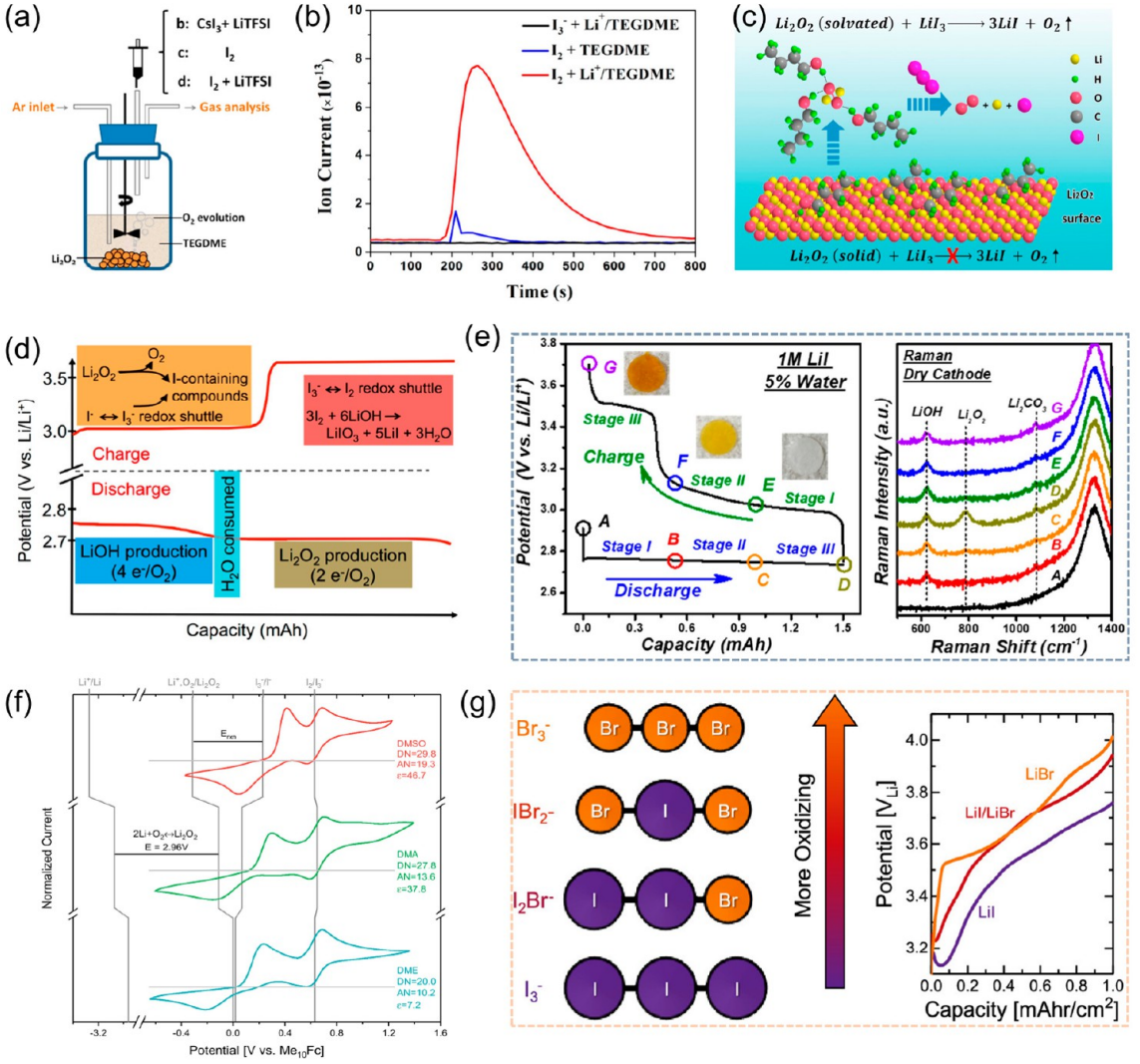

Figure 13. (a, b) Mass spectrometry on the chemical reactivity of oxidized I^- (I_3^-, I_2) with Li_2O_2: schematic illustration of the mass spectrometry process (a) and oxygen analysis carried out after the injection of 100 mM CsI_3 + 1 M LiTFSI/TEGDME, 100 mM I_2 TEGDME, and 100 mM I_2 + 1 M LiTFSI TEGDME solution into the Ar-filled glass vial containing commercial Li_2O_2 powder and TEGDME (b). Reproduced with permission from ref 119. Copyright 2016 American Chemical Society. (c) Schematic exhibiting the enhanced reaction kinetics between LiI_3 and Li_2O_2 by solvating Li_2O_2. Reproduced with permission from ref 121. Copyright 2017 Elsevier. (d) Discharge/charge curves and the corresponding reactions in the LOBs containing LiI and H_2O. Reproduced with permission from ref 68. Copyright 2016 American Chemical Society. (e) Voltage profile with the selected stages marked by specific colors (left) and the corresponding Raman spectra (right). The photos in the inset present the separator collected during charging, which reflects the color change of LiI-contained electrolyte at the corresponding charge stages: I^- (no color), I_3^- (golden yellow), and I_2 (brown). Reproduced with permission from ref 73. Copyright 2017 American Chemical Society. (f) Cyclic voltammograms of solutions of 0.5 M LiTFSI + 10 mM LiI collected at 100 mV/s under an Ar environment in each of the considered solvents with a Pt working electrode, either Li metal (DME, DMSO) or lithium titanium oxide (DMA) counter electrode, and Ag/Ag^+ reference electrode. Reproduced with permission from ref 124. Copyright 2019 Elsevier. (g) Redox potentials of different inter-halides. Reproduced with permission from ref 125. Copyright 2022 American Chemical Society.

noting that even in nominally anhydrous electrolytes (usually determined by Karl Fischer titration), H_2O could come from other components of the cell, like separators, and therefore all cell components should be carefully dried before use to create a truly dry condition. At the end, if both electrolyte solvent and H_2O can serve as the proton provider, the use of H_2O would circumvent the decomposition of the solvent, which is beneficial for enhancing the battery performance on the condition that corrosion of the Li anode by H_2O can be prevented.

What is the true species that triggers the solvent/H_2O deprotonation? In aprotic LOBs, O_2 molecules are first reduced to the reactive superoxide radicals, which are believed to cause the deprotonation of the ether-based electrolytes or H_2O by nucleophilic attack and then generate hydroperoxide intermediates.[73,114] Additionally, through evaluating the deprotonation capability of IO_3^-, formed by the reaction between I^- and O_2 and other nucleophiles (IO^-, Li_2O_2, O_2^-, LiO_2, and $^1O_2$) present in the LOBs, in the three common solvents (DMSO, ACN, and DME) (Figure 12b), Wang et al. suggested that IO_3^- was the only nucleophile that can trigger spontaneous solvent deprotonation.[115] This also explained why the cells containing LiBr additives, which did not tend to form BrO_3^-, were not able to generate LiOH. Additionally, it was proposed that, compared to O_2^-, the products (small aggregates/clusters of LiO_2-like and

https://doi.org/10.1021/cbe.4c00025
Chem Bio Eng. 2024, 1, 737−756

Li_2O_2-like species) generated by the disproportionation of O_2^- were the main oxidants for the deprotonation of H_2O.[74] Considering the high complexity in the LOBs, it is difficult to accurately identify the true species involved in the LiOH chemistry, and some advanced *in situ* technologies (e.g., UV-vis and Raman) yet to be demonstrated may be helpful.[19,73,116]

What is the LiOH formation mechanism mediated by the I-based species? It was claimed by Tułodziecki et al. that I^- can mediate the decomposition of H_2O_2, the intermediate in the transformation process of Li_2O_2 to LiOH (as shown in eqs 7 and 8, Figure 12c).[74]

$$Li_2O_2 + 2H_2O \rightarrow H_2O_2 + 2LiOH \quad (7)$$

$$H_2O_2 + 3I^- + 2Li^+ \rightarrow 2LiOH + I_3^- \quad (8)$$

However, Qiao et al. showed that the initial discharge product was HO_2^- and IO^- species were detected by UV-vis during discharge. They thus claimed that it is the I^-/IO^- couple that induces the O−O cleavage for the formation of LiOH (as shown in eqs 9 and 10, Figure 12d).[73]

$$HO_2^- + I^- \rightarrow IO^- + OH^- \quad (9)$$

$$IO^- + HO_2^- \rightarrow OH^- + O_2 + I^- \quad (10)$$

The ORR process in the aprotic media with limited H_2O additives can be summarized as shown in eqs 11−14).[19,117]

$$2O_2 + 2e^- \rightarrow 2O_2^- \quad (11)$$

$$2O_2^- + H_2O \rightarrow HO_2^- + OH^- + O_2 \quad (12)$$

$$HO_2^- + OH^- + 2Li^+ \leftrightarrow Li_2O_2 + H_2O \quad (13)$$

$$HO_2^- + H_2O \rightarrow H_2O_2 + OH^- \quad (14)$$

Therefore, the I-catalyzed H_2O_2 and HO_2^- decomposition pathways could both contribute to the generation of LiOH. On the other hand, it is still unclear whether I^-/I_3^- redox or I/IO^- redox is responsible for the above pathways. Both I_3^- and IO^- were detected by Qiao et al.,[73] but only I_3^- was observed by Liu et al.[118] It is worth noting that IO^- is unstable and easy to transform into other I-based species (e.g., I_3^-). Therefore, I/IO^- may be the primary redox couple involved in the discharge process.

Why were miscellaneous discharge products generated in the electrolyte with high H_2O content? It is commonly agreed that the more H_2O is added, the more feasible it becomes to form LiOH because of the enrichment of the proton source. However, several works all found that the discharge product changed from LiOH to Li_2O_2, $LiOH·H_2O$, or $LiOOH·H_2O$ in the high-H_2O-content systems with LiI additives. Tułodziecki et al. suggested that, at low H_2O:LiI ratio, the acidity of the H_2O proton was enhanced by a strong iodide−H_2O interaction, which promoted the protonation of LiO_2/Li_2O_2 and thus facilitated the LiOH formation (Figure 12c and eqs 7 and 8).[74] However, at high H_2O:LiI ratio, the H_2O acidity was decreased as the iodide−H_2O interaction was weakened, leading to the formation of $LiOH·H_2O$ rather than H_2O_2 by the reactions of Li_2O_2 and H_2O (eqs 15 and 16).

$$Li_2O_2 + 3H_2O \rightarrow LiOOH·H_2O + LiOH·H_2O \quad (15)$$

$$2LiOOH·H_2O \rightarrow 2LiOH·H_2O + O_2 \quad (16)$$

Liu et al. corroborated the existence of the iodide−H_2O interaction via the hydrogen−halogen bonding at the low H_2O content (<5%) (Figure 12e).[118] Nevertheless, the iodide anions were strongly coordinated by the large $LiI·H_2O$ clusters when the H_2O content was increased to 5%, as indicated by the molecular dynamics simulation (Figure 12f). As a result, the catalytic function of I^- for decomposing H_2O_2 was retarded with both Li_2O_2 and LiOH generation (Figure 12c). On the other side, Qiao et al. claimed that the alkalinity was increased with increasing H_2O content, which could stabilize the HO_2^- intermediates to turn back to the Li_2O_2 discharge product (Figure 12d).[73] Notably, the initial discharge product in the work of Qiao et al. was LiOH at the H_2O content of 5%, suggesting the uninfluenced catalytic effect of I^- in the real battery testing conditions. Therefore, the exact H_2O content above which the catalytic effect of I^- will be hindered needs further clarification.

4.4. Controversies on Charge. The high round-trip efficiency, rate performance, and long cycle life of the LiI-containing LOBs with Li_2O_2/LiOH as the energy carriers show promise for practical applications. However, some doubts have also been raised, including whether I^-/I_3^- could enable the oxidation of Li_2O_2/LiOH and how reversible the charge process is.

Could I^-/I_3^- enable the oxidation of Li_2O_2/LiOH? First, for the oxidation of Li_2O_2, I^-/I_3^- was shown to oxidize Li_2O_2 in TEGDME because only the first charge plateau (assigned to I^-/I_3^-) appeared.[38] Later, Li et al. argued that Li_2O_2 particles in TEGDME could only be chemically oxidized by I_2 rather than I_3^-, considering the quite slow reaction kinetics between I_3^- and Li_2O_2 particles (Figure 13a,b).[119] Kim et al. presented similar results, but they additionally suggested that I_3^-/Br_3^- can oxidize the electrochemically generated Li_2O_2.[120] Zhang et al. claimed that the reaction kinetics between the oxidized RM and Li_2O_2 were affected by the surface properties, as the solvated Li_2O_2 showed faster kinetics than solid Li_2O_2 when reacting with LiI_3 (Figure 13c).[121] As for the decomposition of LiOH, Liu et al. demonstrated that LiOH could be removed by I^-/I_3^- redox and the battery showed excellent reversibility.[41] However, Viswanathan et al. commented that the I^-/I_3^- couple (with the redox potential at about 3.0 V) was unable to oxidize LiOH (with the equilibrium potential of about 3.4 V) from the thermodynamic standpoint.[122] Additionally, Shen et al. expressed the same concern because the accumulation of I_3^- in the electrolyte was observed through a transparent cell.[123] Therefore, they suggested that the reaction during the charge process was I^- to I_3^- rather than the decomposition of LiOH. Burke et al. revealed that, in the DME-based electrolyte with 0.05/0.2 M LiI, LiOH could not be removed at the charge plateau of 3.0 V but could be realized at 3.5 V, assigned to the redox potential of I_3^-/I_2 (Figure 13d).[68] Qiao et al. also suggested that both I^-/I_3^- and I_3^-/I_2 failed to oxidize LiOH in TEGDME-based electrolyte with 1 M LiI and 5% H_2O, as supported by the dyed separator and the residual LiOH after charging (Figure 13e).[73] All the above results emphasized that I^-/I_3^- was unable to decompose LiOH, which was inconsistent with the results from Liu et al. Actually, the different redox potentials of I^-/I_3^- and $LiOH/O_2$ and the different surface properties of LiOH, caused by the discrepancies in the cathode materials, H_2O contents, or LiI concentrations, could lead to the inconsistent observations in the above works. In order to improve the oxidizing ability of the I^-/I_3^- couple and avoid the occurrence of the more oxidizing I_2, some measures were proposed. First, the degree of I^- solvation in a solvent affects the redox potential of I^-/I_3^- and thus influences its oxidizing ability (Figure 13f). As a result, the I^-/I_3^-

https://doi.org/10.1021/cbe.4c00025
Chem Bio Eng. 2024, 1, 737−756

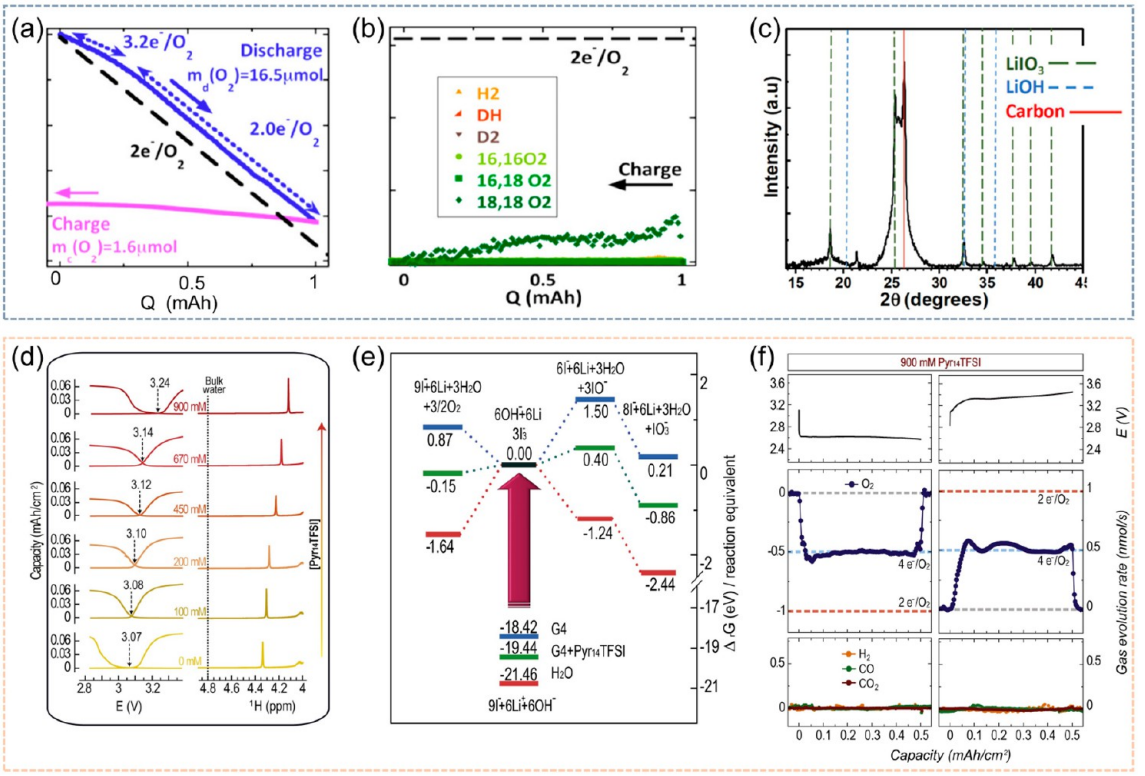

Figure 14. (a, b) Galvanostatic discharge and charge profiles (100 μA/cm^2) with oxygen consumption and gas evolution for LOBs with the electrolyte containing 0.2 M LiI and 5000 ppm of H_2O. (c) XRD patterns for the cycled cathode in the LOB with LiI and H_2O additives, showing the depositition of $LiIO_3$. Reproduced with permission from ref 68. Copyright 2016 American Chemical Society. (d) Effect of $Pyr_{14}TFSI$ concentration (0−900 mM) on galvanostatic charge/discharge curves (left), and solution ^1H NMR of 700 mM LiTFSI, 50 mM LiI, and 5000 ppm of H_2O in G4 electrolyte (right). (e) Free-energy diagram for the proposed mechanisms involving the iodide-mediated LiOH oxidation (O_2 evolution [left] and IO^- and IO_3^- formation [right], relative to I_3^- formation in G4 [blue], G4 + 900 mM $Pyr_{14}TFSI$ [green], and H_2O [red]). (f) Galvanostatic profiles (top) and online mass spectrometry analysis of O_2 (middle) and H_2, CO, and CO_2 (bottom) from batteries with electrolytes comprising 700 mM LiTFSI, 50 mM LiI, and 5000 ppm of H_2O in G4 with 900 mM $Pyr_{14}TFSI$ cycled at a current of 50 μA/cm^2. Reproduced with permission from ref 126. Copyright 2020 Elsevier.

couple was capable of removing Li_2O_2/LiOH in the solvents (e.g., DMSO, *N,N*-dimethylacetamide (DMA), and 1-methylimidazole (Me-Im)) with high Guttmann acceptor number (AN) but not in the solvents (e.g., DME, TEGDME) with lower AN.[124] In addition, forming the inter-halide RMs based on LiI/LiBr and LiI/LiCl mixtures could also tune the oxidizing power of LiX in a given solvent (Figure 13g).[125]

How reversible is the charge process? Since the LiOH formation is through a stoichiometric 4e$^-$ ORR ($4Li^+ + H_2O + O_2 + 4e^- \rightarrow 4LiOH$), the reversible decomposition of LiOH should accordingly be a stoichiometric 4e$^-$ OER ($4LiOH \rightarrow 4Li^+ + H_2O + O_2 + 4e^-$). Some works indeed detected the oxygen gas evolution by mass spectrometry in a LiOH-preloaded battery with LiI additives or in a vessel containing I_2, and 2 M LiOH suspension in DME/H_2O (10:1), but the oxygen evolution was not quantified.[41,69] On the other hand, some other works monitored the gas evolution during charge by differential electrochemical mass spectrometry (DEMS), but no signal of O_2 was obtained. Instead, IO_3^- was detected (Figure 14a−c), and thus the researchers proposed that the reaction during charge was $3I_2 + 6LiOH \rightarrow 5LiI + LiIO_3 + 3H_2O$.[68] The transformation from LiOH to O_2 and that from LiOH to $LiIO_3$ should be two competing pathways. The generation of $LiIO_3$ is thermodynamically preferred, while the generation of O_2 needs to overcome a kinetic barrier associated with O−O bond formation.[90] As a result, the oxygen in LiOH is usually trapped in $LiIO_3$ rather than being liberated. As for the decomposition of Li_2O_2, the situation is reversed relative to that for LiOH as the O−O bond is maintained in Li_2O_2, which makes the O_2 evolution more favored compared to the production of $LiIO_3$ during charge. As the I species trapped in $LiIO_3$ would lose its catalytic activity after mediating the decomposition of LiOH, LiI was not considered as a proper RM in the LiOH chemistry. Recently, Temprano et al. fulfilled the reversibility of a LiOH-based battery through elaborate design of the electrolyte.[126] In their battery system, the electrolyte consists of TEGDME, 0.7 M LiTFSI, 50 mM LiI, 5000 ppm of H_2O, and 900 mM *N*-butyl-*N*-methylpyrrolidinium bis((trifluoromethyl)sulfonyl)imide ($Pyr_{14}TFSI$). The introduction of $Pyr_{14}TFSI$ was beneficial for increasing the solvation of I^- and H_2O, and the redox potential of I^-/I_3^- was raised from 3.07 to 3.24 V after addition of 900 mM $Pyr_{14}TFSI$ (Figure 14d). Additionally, IO^- formation during charge became disfavored in the presence of $Pyr_{14}TFSI$, evidenced by DFT calculations, leading to O_2 evolution without the generation of $LiIO_3$ during charge (Figure 14e). Consequently, the battery showed a low initial charge potential at 3.1 V, a charge plateau at 3.4 V, and a remarkable faradaic efficiency of 99.5% (Figure 14f). However, the faradaic efficiency decreased to 80% after 7 cycles, indicating the occurrence of some parasite reactions. The long-term cycling of this battery was yet to be demonstrated. In conclusion, the oxidation of Li_2O_2 mediated by LiI is usually reversible with O_2

https://doi.org/10.1021/cbe.4c00025
Chem Bio Eng. 2024, 1, 737−756

evolution; in contrast, the decomposition of LiOH induced by LiI is accompanied by the formation of $LiIO_3$, which would destroy the cyclability of I species and thus the cycle performance of the batteries. Optimizing the recipe for the electrolyte is a promising method to achieve a highly reversible LiOH-based battery, but the design principle is still lacking.

5. CONCLUSIONS AND PERSPECTIVES

In this Review, we have summarized various functions of HRMs in LOBs and additionally analyzed the main challenges and controversies confronted by HRMs. Although evident enhancements in LOBs in terms of round-trip efficiency, power/energy density, and cycle life have been achieved with the assistance of HRMs, notable breakthroughs in the following aspects are still desired to satisfy the requirements for practical applications.

(i) *Expanding the HRMs library*. Compared to LiX with a single function, organo-halogen compounds with unique cations can optimize simultaneously the key components in LOBs. However, the candidates are still sparse and the SEI layers created by the reported additives are either heterogeneous or organic-dominant, which are easily destroyed during cycling. We can resort to high-throughput computational screening for selecting ideal organic cations that can enable the construction of homogeneous and mechanically stable SEIs.[127] On the other hand, versatile F-containing additives are also intriguing yet receive less attention in LOBs.[128]

(ii) *Combining HRMs with advanced cathodes*. The cathode can be complementary with the additives in promoting the decomposition of discharge products and side products.[129] Also, the porous cathode can enable the fast diffusion of soluble additives to enhance the rate performance and oxidation efficiency.[41] In addition, a well-designed cathode with functional groups can hinder the redox shuttling by physical confinement or chemisorption and even serve as a slow-release capsule to prolong the efficacy of halide additives.[130]

(iii) *Designing the solvents matched well with HRMs*. Ethers (e.g., TEGDME) are the most prevalent solvents in LOBs because of their stability toward nucleophiles and excellent compatibility with the Li anode.[131] Nevertheless, the low DN and the high viscosity of TEGDME decrease the oxidizing ability and the diffusion of HRMs. DMSO, with higher DN and lower viscosity, is an alternative to offset the shortcomings of TEGDME, but it suffers from nucleophilic attack and is not compatible with Li anode.[132] Therefore, developing advanced electrolyte systems (e.g., mixed electrolyte) matched well with HRMs is urgent, yet less progress has been achieved.

(iv) *Studying the OER kinetics in HRMs-mediated LOBs*. The kinetics of the electrochemical oxidation of HRMs themselves and the chemical reaction between HRMs and different discharge products determine the performance of LOBs, especially rate performance. However, only a few works have been conducted to study the OER kinetics.[31,36,133,134] Some vital aspects still remain unclear, such as the relationship between the redox potential and OER kinetics and the influence of the morphology and structure of the discharge products on the OER kinetics. Besides, whether the catalysts are necessary to promote the electro-oxidation of X^- is also questionable.

(v) *Developing long-lasting and reversible LiOH-based LOBs*. LiI-mediated LiOH chemistry is promising for the practical application of LOBs, but the oxidizing ability of I_3^- and the reversibility of the OER process seem unsatisfied. Modifying the formula of the electrolyte regarding the selection of solvent with high DN or introducing some special ionic liquid additives would be useful. Further works are still needed to demonstrate the true reversibility of the LiOH-based LOBs catalyzed by RMs or solid catalysts. Additionally, the influence of H_2O on the LiOH chemistry is also elusive, especially when the content of H_2O changes during the battery operation. To alleviate this issue, introducing moisture O_2 as the reactant and investigating with various advanced spectrum techniques are recommended.

Overall, developing high-performance LOBs calls for systematic works on additives, anodes, cathodes, and electrolytes with the help of the cutting-edge characterization techniques and theoretical studies.

AUTHOR INFORMATION

Corresponding Author

Huilong Fei − *Advanced Catalytic Engineering Research Center of the Ministry of Education, State Key Laboratory for Chemo/Biosensing and Chemometrics, and College of Chemistry and Chemical Engineering, Hunan University, Changsha 410082, China*; orcid.org/0000-0002-4216-5810; Email: hlfei@hnu.edu.cn

Authors

Kang Huang − *Advanced Catalytic Engineering Research Center of the Ministry of Education, State Key Laboratory for Chemo/Biosensing and Chemometrics, and College of Chemistry and Chemical Engineering, Hunan University, Changsha 410082, China*

Zhixiu Lu − *Advanced Catalytic Engineering Research Center of the Ministry of Education, State Key Laboratory for Chemo/Biosensing and Chemometrics, and College of Chemistry and Chemical Engineering, Hunan University, Changsha 410082, China*

Shilong Dai − *Advanced Catalytic Engineering Research Center of the Ministry of Education, State Key Laboratory for Chemo/Biosensing and Chemometrics, and College of Chemistry and Chemical Engineering, Hunan University, Changsha 410082, China*

Complete contact information is available at: https://pubs.acs.org/10.1021/cbe.4c00025

Notes

The authors declare no competing financial interest.

ACKNOWLEDGMENTS

H.F. acknowledges financial support from the National Natural Science Foundation of China (Grant No. 92163116) and Major Program of the Natural Science Foundation of Hunan Province (Grant No. 2021JC0006).

REFERENCES

(1) Zhu, Z.; Jiang, T.; Ali, M.; Meng, Y.; Jin, Y.; Cui, Y.; Chen, W. Rechargeable Batteries for Grid Scale Energy Storage. *Chem. Rev.* **2022**, *122* (22), 16610−16751.

(2) Choi, J. W.; Aurbach, D. Promise and Reality of Post-Lithium-Ion Batteries with High Energy Densities. *Nat. Rev. Mater.* **2016**, *1* (4), 16013.
(3) Lu, Y. C.; Gallant, B. M.; Kwabi, D. G.; Harding, J. R.; Mitchell, R. R.; Whittingham, M. S.; Shao-Horn, Y. Lithium-Oxygen Batteries: Bridging Mechanistic Understanding and Battery Performance. *Energy Environ. Sci.* **2013**, *6* (3), 750−768.
(4) Cheng, X. B.; Zhang, R.; Zhao, C. Z.; Zhang, Q. Toward Safe Lithium Metal Anode in Rechargeable Batteries: A Review. *Chem. Rev.* **2017**, *117* (15), 10403−10473.
(5) Jin, C. B.; Liu, T. F.; Sheng, O. W.; Li, M.; Liu, T. C.; Yuan, Y. F.; Nai, J. W.; Ju, Z. J.; Zhang, W. K.; Liu, Y. J.; et al. Rejuvenating Dead Lithium Supply in Lithium Metal Anodes by Iodine Redox. *Nat. Energy* **2021**, *6* (4), 378−387.
(6) Aurbach, D.; McCloskey, B. D.; Nazar, L. F.; Bruce, P. G. Advances in Understanding Mechanisms Underpinning Lithium-Air Batteries. *Nat. Energy* **2016**, *1* (9), 16128.
(7) Bruce, P. G.; Freunberger, S. A.; Hardwick, L. J.; Tarascon, J. M. Li-O_2 and Li-S Batteries with High Energy Storage. *Nat. Mater.* **2012**, *11* (1), 19−29.
(8) Kwak, W. J.; Rosy; Sharon, D.; Xia, C.; Kim, H.; Johnson, L. R.; Bruce, P. G.; Nazar, L. F.; Sun, Y. K.; Frimer, A. A.; et al. Lithium-Oxygen Batteries and Related Systems: Potential, Status, and Future. *Chem. Rev.* **2020**, *120* (14), 6626−6683.
(9) Liu, T.; Vivek, J. P.; Zhao, E. W.; Lei, J.; Garcia-Araez, N.; Grey, C. P. Current Challenges and Routes Forward for Nonaqueous Lithium-Air Batteries. *Chem. Rev.* **2020**, *120* (14), 6558−6625.
(10) Cao, R. F.; Chen, K.; Liu, J. W.; Huang, G.; Liu, W. Q.; Zhang, X. B. Li-air batteries: air stability of lithium metal anodes. *Sci. China Chem.* **2024**, *67*, 122.
(11) Kang, J. H.; Lee, J.; Jung, J. W.; Park, J.; Jang, T.; Kim, H. S.; Nam, J. S.; Lim, H.; Yoon, K. R.; Ryu, W. H.; et al. Lithium-Air Batteries: Air-Breathing Challenges and Perspective. *ACS Nano* **2020**, *14* (11), 14549−14578.
(12) Li, F. J.; Chen, J. Mechanistic Evolution of Aprotic Lithium-Oxygen Batteries. *Adv. Energy Mater.* **2017**, *7* (24), 1602934.
(13) Shu, C.; Wang, J.; Long, J.; Liu, H. K.; Dou, S. X. Understanding the Reaction Chemistry during Charging in Aprotic Lithium-Oxygen Batteries: Existing Problems and Solutions. *Adv. Mater.* **2019**, *31* (15), No. e1804587.
(14) Zhang, P.; Ding, M. J.; Li, X. X.; Li, C. X.; Li, Z. Q.; Yin, L. W. Challenges and Strategy on Parasitic Reaction for High-Performance Nonaqueous Lithium-Oxygen Batteries. *Adv. Energy Mater.* **2020**, *10* (40), 202001789.
(15) McCloskey, B. D.; Addison, D. A Viewpoint on Heterogeneous Electrocatalysis and Redox Mediation in Nonaqueous Li-O_2 Batteries. *ACS Catal.* **2017**, *7* (1), 772−778.
(16) Li, J. T.; Bi, X. X.; Amine, K.; Lu, J. Understanding the Effect of Solid Electrocatalysts on Achieving Highly Energy-Efficient Lithium-Oxygen Batteries. *Adv. Energy Sustainability Res.* **2021**, *2* (9), 2100045.
(17) Ko, Y.; Park, H.; Kim, B.; Kim, J. S.; Kang, K. Redox Mediators: A Solution for Advanced Lithium-Oxygen Batteries. *Trends Chem.* **2019**, *1* (3), 349−360.
(18) Black, R.; Oh, S. H.; Lee, J. H.; Yim, T.; Adams, B.; Nazar, L. F. Screening for superoxide reactivity in Li-O_2 batteries: effect on Li_2O_2/LiOH crystallization. *J. Am. Chem. Soc.* **2012**, *134* (6), 2902−2905.
(19) Qiao, Y.; Wu, S.; Yi, J.; Sun, Y.; Guo, S.; Yang, S.; He, P.; Zhou, H. From O_2^- to HO_2^-: Reducing By-Products and Overpotential in Li-O_2 Batteries by Water Addition. *Angew. Chem. Int. Ed.* **2017**, *56* (18), 4960−4964.
(20) Lim, H. D.; Lee, B.; Bae, Y.; Park, H.; Ko, Y.; Kim, H.; Kim, J.; Kang, K. Reaction Chemistry in Rechargeable Li-O_2 Batteries. *Chem. Soc. Rev.* **2017**, *46* (10), 2873−2888.
(21) Park, J. B.; Lee, S. H.; Jung, H. G.; Aurbach, D.; Sun, Y. K. Redox Mediators for Li-O_2 Batteries: Status and Perspectives. *Adv. Mater.* **2018**, *30* (1), 1704162.
(22) Chen, Y.; Freunberger, S. A.; Peng, Z.; Fontaine, O.; Bruce, P. G. Charging a Li-O_2 Battery Using a Redox Mediator. *Nat. Chem.* **2013**, *5* (6), 489−494.
(23) Bergner, B. J.; Schurmann, A.; Peppler, K.; Garsuch, A.; Janek, J. TEMPO: A Mobile Catalyst for Rechargeable Li-O_2 Batteries. *J. Am. Chem. Soc.* **2014**, *136* (42), 15054−15064.
(24) Kwak, W.-J.; Kim, H.; Jung, H.-G.; Aurbach, D.; Sun, Y.-K. Review—A Comparative Evaluation of Redox Mediators for Li-O_2 Batteries: A Critical Review. *J. Electrochem. Soc.* **2018**, *165* (10), A2274−A2293.
(25) Zhang, C. J.; Dandu, N.; Rastegar, S.; Misal, S. N.; Hemmat, Z.; Ngo, A. T.; Curtiss, L. A.; Salehi-Khojin, A. A Comparative Study of Redox Mediators for Improved Performance of Li-Oxygen Batteries. *Adv. Energy Mater.* **2020**, *10* (27), 2000201.
(26) Lim, H. D.; Lee, B.; Zheng, Y.; Hong, J.; Kim, J.; Gwon, H.; Ko, Y.; Lee, M.; Cho, K.; Kang, K. Rational Design of Redox Mediators for Advanced Li-O_2 Batteries. *Nat. Energy* **2016**, *1* (6), 16066.
(27) Dou, Y.; Xie, Z.; Wei, Y.; Peng, Z.; Zhou, Z. Redox Mediators for High-Performance Lithium-Oxygen Batteries. *Natl. Sci. Rev.* **2022**, *9* (4), nwac040.
(28) Lin, X. D.; Yuan, R. M.; Cao, Y.; Ding, X. B.; Cai, S. R.; Han, B. W.; Hong, Y. H.; Zhou, Z. Y.; Yang, X. L.; Gong, L.; et al. Controlling Reversible Expansion of Li_2O_2 Formation and Decomposition by Modifying Electrolyte in Li-O_2 Batteries. *Chem.* **2018**, *4* (11), 2685−2698.
(29) Li, J. J.; Ding, S. Q.; Zhang, S. M.; Yan, W.; Ma, Z. F.; Yuan, X. X.; Mai, L. Q.; Zhang, J. J. Catalytic Redox Mediators for Non-Aqueous Li-O_2 Battery. *Energy Stor. Mater.* **2021**, *43*, 97−119.
(30) Askins, E. J.; Zoric, M. R.; Li, M.; Amine, R.; Amine, K.; Curtiss, L. A.; Glusac, K. D. Triarylmethyl Cation Redox Mediators Enhance Li-O_2 Battery Discharge Capacities. *Nat. Chem.* **2023**, *15* (9), 1247−1254.
(31) Ko, Y.; Kim, K.; Yoo, J.; Kwon, G.; Park, H.; Kim, J.; Lee, B.; Song, J. H.; Kim, J.; Kang, K. Redox Mediators for Oxygen Reduction Reactions in Lithium-Oxygen Batteries: Governing Kinetics and Its Implications. *Energy Environ. Sci.* **2023**, *16* (11), 5525−5533.
(32) Ryu, W. H.; Gittleson, F. S.; Thomsen, J. M.; Li, J.; Schwab, M. J.; Brudvig, G. W.; Taylor, A. D. Heme Biomolecule as Redox Mediator and Oxygen Shuttle for Efficient Charging of Lithium-Oxygen Batteries. *Nat. Commun.* **2016**, *7*, 12925.
(33) Nishioka, K.; Morimoto, K.; Kusumoto, T.; Harada, T.; Kamiya, K.; Mukouyama, Y.; Nakanishi, S. Isotopic Depth Profiling of Discharge Products Identifies Reactive Interfaces in an Aprotic Li-O_2 Battery with a Redox Mediator. *J. Am. Chem. Soc.* **2021**, *143* (19), 7394−7401.
(34) Dou, Y.; Kan, D.; Su, Y.; Zhang, Y.; Wei, Y.; Zhang, Z.; Zhou, Z. Critical Factors Affecting the Catalytic Activity of Redox Mediators on Li-O_2 Battery Discharge. *J. Phys. Chem. Lett.* **2022**, *13* (30), 7081−7086.
(35) Xing, S. C.; Zhang, Z. C.; Dou, Y. Y.; Li, M. H.; Wu, J.; Zhang, Z.; Zhou, Z. An Efficient Multifunctional Soluble Catalyst for Li-O_2 Batteries. *CCS Chem.* **2023**, 1.
(36) Ko, Y.; Park, H.; Lee, B.; Bae, Y.; Park, S. K.; Kang, K. A Comparative Kinetic Study of Redox Mediators for High-Power Lithium-Oxygen Batteries. *J. Mater. Chem. A* **2019**, *7* (11), 6491−6498.
(37) Kwak, W. J.; Hirshberg, D.; Sharon, D.; Afri, M.; Frimer, A. A.; Jung, H. G.; Aurbach, D.; Sun, Y. K. Li-O_2 Cells With LiBr as an Electrolyte and a Redox Mediator. *Energy Environ. Sci.* **2016**, *9* (7), 2334−2345.
(38) Lim, H. D.; Song, H.; Kim, J.; Gwon, H.; Bae, Y.; Park, K. Y.; Hong, J.; Kim, H.; Kim, T.; Kim, Y. H.; et al. Superior Rechargeability and Efficiency of Lithium-Oxygen Batteries: Hierarchical Air Electrode Architecture Combined with a Soluble Catalyst. *Angew. Chem. Int. Ed.* **2014**, *53* (15), 3926−3931.
(39) Zhao, Q.; Katyal, N.; Seymour, I. D.; Henkelman, G.; Ma, T. Vanadium(III) Acetylacetonate as an Efficient Soluble Catalyst for Lithium-Oxygen Batteries. *Angew. Chem. Int. Ed.* **2019**, *58* (36), 12553−12557.
(40) Lin, X.; Sun, Z.; Tang, C.; Hong, Y.; Xu, P.; Cui, X.; Yuan, R.; Zhou, Z.; Zheng, M.; Dong, Q. Highly Reversible O_2 Conversions by Coupling LiO_2 Intermediate through a Dual-Site Catalyst in Li-O_2 Batteries. *Adv. Energy Mater.* **2020**, *10* (38), 2001592.
(41) Liu, T.; Leskes, M.; Yu, W.; Moore, A. J.; Zhou, L.; Bayley, P. M.; Kim, G.; Grey, C. P. Cycling Li-O_2 Batteries via LiOH Formation and Decomposition. *Science* **2015**, *350* (6260), 530−533.

https://doi.org/10.1021/cbe.4c00025
Chem Bio Eng. 2024, 1, 737−756

(42) Liang, Z.; Lu, Y. C. Critical Role of Redox Mediator in Suppressing Charging Instabilities of Lithium-Oxygen Batteries. *J. Am. Chem. Soc.* **2016**, *138* (24), 7574−7583.
(43) Choudhury, S.; Wan, C. T.; Al Sadat, W. I.; Tu, Z.; Lau, S.; Zachman, M. J.; Kourkoutis, L. F.; Archer, L. A. Designer Interphases for the Lithium-Oxygen Electrochemical Cell. *Sci. Adv.* **2017**, *3* (4), No. e1602809.
(44) Zhang, X. P.; Sun, Y. Y.; Sun, Z.; Yang, C. S.; Zhang, T. Anode Interfacial Layer Formation via Reductive Ethyl Detaching of Organic Iodide in Lithium-Oxygen Batteries. *Nat. Commun.* **2019**, *10* (1), 3543.
(45) Tamirat, A. G.; Guan, X.; Liu, J.; Luo, J.; Xia, Y. Redox Mediators as Charge Agents for Changing Electrochemical Reactions. *Chem. Soc. Rev.* **2020**, *49* (20), 7454−7478.
(46) Zhang, P.; Zhao, Y.; Zhang, X. Functional and Stability Orientation Synthesis of Materials and Structures in Aprotic Li-O_2 Batteries. *Chem. Soc. Rev.* **2018**, *47* (8), 2921−3004.
(47) Xia, Q.; Li, D.; Zhao, L.; Wang, J.; Long, Y.; Han, X.; Zhou, Z.; Liu, Y.; Zhang, Y.; Li, Y.; et al. Recent Advances in Heterostructured Cathodic Electrocatalysts for Non-Aqueous Li-O_2 Batteries. *Chem. Sci.* **2022**, *13* (10), 2841−2856.
(48) Wu, Z.; Tian, Y.; Chen, H.; Wang, L.; Qian, S.; Wu, T.; Zhang, S.; Lu, J. Evolving Aprotic Li-Air Batteries. *Chem. Soc. Rev.* **2022**, *51* (18), 8045−8101.
(49) Wang, Y.; Lu, Y. C. Nonaqueous Lithium-Oxygen Batteries: Reaction Mechanism and Critical Open Questions. *Energy Stor. Mater.* **2020**, *28*, 235−246.
(50) Mahne, N.; Fontaine, O.; Thotiyl, M. O.; Wilkening, M.; Freunberger, S. A. Mechanism and Performance of Lithium-Oxygen Batteries—a Perspective. *Chem. Sci.* **2017**, *8* (10), 6716−6729.
(51) Johnson, L.; Li, C.; Liu, Z.; Chen, Y.; Freunberger, S. A.; Ashok, P. C.; Praveen, B. B.; Dholakia, K.; Tarascon, J. M.; Bruce, P. G. The Role of LiO_2 Solubility in O_2 Reduction in Aprotic Solvents and Its Consequences for Li-O_2 Batteries. *Nat. Chem.* **2014**, *6* (12), 1091−1099.
(52) Peng, Z.; Chen, Y.; Bruce, P. G.; Xu, Y. Direct Detection of the Superoxide Anion as a Stable Intermediate in the Electroreduction of Oxygen in a Non-Aqueous Electrolyte Containing Phenol as a Proton Source. *Angew. Chem. Int. Ed.* **2015**, *54* (28), 8165−8168.
(53) Mahne, N.; Schafzahl, B.; Leypold, C.; Leypold, M.; Grumm, S.; Leitgeb, A.; Strohmeier, G. A.; Wilkening, M.; Fontaine, O.; Kramer, D.; et al. Singlet Oxygen Generation as a Major Cause for Parasitic Reactions during Cycling of Aprotic Lithium-Oxygen Batteries. *Nat. Energy* **2017**, *2* (5), 17036.
(54) Lu, J.; Lei, Y.; Lau, K. C.; Luo, X.; Du, P.; Wen, J.; Assary, R. S.; Das, U.; Miller, D. J.; Elam, J. W.; et al. A Nanostructured Cathode Architecture For Low Charge Overpotential in Lithium-Oxygen Batteries. *Nat. Commun.* **2013**, *4*, 2383.
(55) Qiao, Y.; Jiang, K. Z.; Deng, H.; Zhou, H. S. A High-Energy-Density and Long-Life Lithium-Ion Battery via Reversible Oxide-Peroxide Conversion. *Nat. Catal.* **2019**, *2* (11), 1035−1044.
(56) Xia, C.; Kwok, C. Y.; Nazar, L. F. A High-Energy-Density Lithium-Oxygen Battery Based on a Reversible Four-Electron Conversion to Lithium Oxide. *Science* **2018**, *361* (6404), 777−781.
(57) Zhang, G.; Li, G.; Wang, J.; Tong, H.; Wang, J.; Du, Y.; Sun, S.; Dang, F. 2D SnSe Cathode Catalyst Featuring an Efficient Facet-Dependent Selective Li_2O_2 Growth/Decomposition for Li-Oxygen Batteries. *Adv. Energy Mater.* **2022**, *12* (21), 2103910.
(58) Lv, Q.; Zhu, Z.; Ni, Y.; Geng, J.; Li, F. Spin-State Manipulation of Two-Dimensional Metal-Organic Framework with Enhanced Metal-Oxygen Covalency for Lithium-Oxygen Batteries. *Angew. Chem. Int. Ed.* **2022**, *61* (8), No. e202114293.
(59) Xu, S. M.; Zhu, Q. C.; Harris, M.; Chen, T. H.; Ma, C.; Wei, X.; Xu, H. S.; Zhou, Y. X.; Cao, Y. C.; Wang, K. X.; et al. Toward Lower Overpotential through Improved Electron Transport Property: Hierarchically Porous CoN Nanorods Prepared by Nitridation for Lithium-Oxygen Batteries. *Nano Lett.* **2016**, *16* (9), 5902−5908.
(60) Li, C.; Wei, J.; Qiu, K.; Wang, Y. Li-air Battery with a Superhydrophobic Li-Protective Layer. *ACS Appl. Mater. Interfaces* **2020**, *12* (20), 23010−23016.
(61) Liu, T.; Feng, X. L.; Jin, X.; Shao, M. Z.; Su, Y. T.; Zhang, Y.; Zhang, X. B. Protecting the Lithium Metal Anode for a Safe Flexible Lithium-Air Battery in Ambient Air. *Angew. Chem. Int. Ed.* **2019**, *58* (50), 18240−18245.
(62) Zhang, X.; Zhang, Q.; Wang, X. G.; Wang, C.; Chen, Y. N.; Xie, Z.; Zhou, Z. An Extremely Simple Method for Protecting Lithium Anodes in Li-O_2 Batteries. *Angew. Chem. Int. Ed.* **2018**, *57* (39), 12814−12818.
(63) Kwak, W. J.; Lau, K. C.; Shin, C. D.; Amine, K.; Curtiss, L. A.; Sun, Y. K. A Mo_2C/Carbon Nanotube Composite Cathode for Lithium-Oxygen Batteries with High Energy Efficiency and Long Cycle Life. *ACS Nano* **2015**, *9* (4), 4129−4137.
(64) Wu, S.; Qiao, Y.; Yang, S.; Ishida, M.; He, P.; Zhou, H. Organic Hydrogen Peroxide-Driven Low Charge Potentials for High-Performance Lithium-Oxygen Batteries with Carbon Cathodes. *Nat. Commun.* **2017**, *8*, 15607.
(65) Kondori, A.; Esmaeilirad, M.; Harzandi, A. M.; Amine, R.; Saray, M. T.; Yu, L.; Liu, T.; Wen, J.; Shan, N.; Wang, H. H.; et al. A Room Temperature Rechargeable Li_2O-Based Lithium-Air Battery Enabled by a Solid Electrolyte. *Science* **2023**, *379* (6631), 499−505.
(66) Lu, J.; Lee, Y. J.; Luo, X.; Lau, K. C.; Asadi, M.; Wang, H. H.; Brombosz, S.; Wen, J.; Zhai, D.; Chen, Z.; et al. A Lithium-Oxygen Battery Based on Lithium Superoxide. *Nature* **2016**, *529* (7586), 377−382.
(67) Wang, L.; Pan, J.; Zhang, Y.; Cheng, X.; Liu, L.; Peng, H. A Li-Air Battery with Ultralong Cycle Life in Ambient Air. *Adv. Mater.* **2018**, *30* (3), 1704378.
(68) Burke, C. M.; Black, R.; Kochetkov, I. R.; Giordani, V.; Addison, D.; Nazar, L. F.; McCloskey, B. D. Implications of 4 e^- Oxygen Reduction via Iodide Redox Mediation in Li-O_2 Batteries. *ACS Energy Lett.* **2016**, *1* (4), 747−756.
(69) Zhu, Y. G.; Liu, Q.; Rong, Y.; Chen, H.; Yang, J.; Jia, C.; Yu, L. J.; Karton, A.; Ren, Y.; Xu, X.; et al. Proton Enhanced Dynamic Battery Chemistry for Aprotic Lithium-Oxygen Batteries. *Nat. Commun.* **2017**, *8* (1), 14308.
(70) Zhang, Q.; Zhou, Y.; Dai, W. R.; Cui, X. H.; Lyu, Z. Y.; Hu, Z.; Chen, W. Chloride Ion as Redox Mediator in Reducing Charge Overpotential of Aprotic Lithium-Oxygen Batteries. *Batteries Supercaps* **2021**, *4* (1), 232−239.
(71) Marques Mota, F.; Kang, J. H.; Jung, Y.; Park, J.; Na, M.; Kim, D. H.; Byon, H. R. Mechanistic Study Revealing the Role of the Br_3^-/Br_2 Redox Couple in CO_2-Assisted Li-O_2 Batteries. *Adv. Energy Mater.* **2020**, *10* (9), 1903486.
(72) Kwak, W. J.; Hirshberg, D.; Sharon, D.; Shin, H. J.; Afri, M.; Park, J. B.; Garsuch, A.; Chesneau, F. F.; Frimer, A. A.; Aurbach, D.; et al. Understanding the Behavior of Li-Oxygen Cells containing LiI. *J. Mater. Chem. A* **2015**, *3* (16), 8855−8864.
(73) Qiao, Y.; Wu, S. C.; Sun, Y.; Guo, S. H.; Yi, J.; He, P.; Zhou, H. S. Unraveling the Complex Role of Iodide Additives in Li-O_2 Batteries. *ACS Energy Lett.* **2017**, *2* (8), 1869−1878.
(74) Tułodziecki, M.; Leverick, G. M.; Amanchukwu, C. V.; Katayama, Y.; Kwabi, D. G.; Bardé, F.; Hammond, P. T.; Shao-Horn, Y. The Role of Iodide in the Formation of Lithium Hydroxide in Lithium-Oxygen Batteries. *Energy Environ. Sci.* **2017**, *10* (8), 1828−1842.
(75) Zhang, T.; Liao, K. M.; He, P.; Zhou, H. S. A Self-Defense Redox Mediator for Efficient Lithium-O_2 Batteries. *Energy Environ. Sci.* **2016**, *9* (3), 1024−1030.
(76) Zhang, C. J.; Jaradat, A.; Singh, S. K.; Rojas, T.; Ahmadiparidari, A.; Rastegar, S.; Wang, S. X.; Majidi, L.; Redfern, P.; Subramanian, A.; et al. Novel Co-Catalytic Activities of Solid and Liquid Phase Catalysts in High-Rate Li-Air Batteries. *Adv. Energy Mater.* **2022**, *12* (45), 202201616.
(77) Liu, J.; Wu, T.; Zhang, S. Q.; Li, D.; Wang, Y.; Xie, H. M.; Yang, J. H.; Sun, G. R. $InBr_3$ as a Self-Defensed Redox Mediator for Li-O_2 Batteries: Construction of a Stable Indium-Rich Composite Protective Layer on the Li Anode. *J. Power Sources* **2019**, *439*, 227095.

https://doi.org/10.1021/cbe.4c00025
Chem Bio Eng. 2024, 1, 737−756

(78) Sun, G.; Wang, Y.; Yang, D.; Zhang, Z.; Lu, W.; Feng, M. Enhanced Cycle Stability of Aprotic Li-O_2 Batteries Based on a Self-Defensed Redox Mediator. *Chin. Chem. Lett.* **2024**, *35* (3), 108469.
(79) Lee, C. K.; Park, Y. J. CsI as Multifunctional Redox Mediator for Enhanced Li-Air Batteries. *ACS Appl. Mater. Interfaces* **2016**, *8* (13), 8561−8567.
(80) Zhang, X. P.; Li, Y. N.; Deng, J. W.; Mao, Y.; Xie, J. Y.; Zhang, T. A Bromo-Nitro Redox Mediator of $BrCH_2NO_2$ for Efficient Lithium-Oxygen Batteries. *J. Power Sources* **2021**, *506*, 230181.
(81) Zheng, C.; Ding, W. W.; Wang, C. N-Methyl-N-Propyl Pyrrolidine Bromide (MPPBr) as a Bi-Functional Redox Mediator for Rechargeable Li-O_2 Batteries. *J. Mater. Chem. A* **2019**, *7* (11), 6180−6186.
(82) Li, C. Y.; Wu, M. S.; Chen, W. R.; Rong, Y. J.; Wang, Q. Y.; Zhang, X. P. Bifunctional Covalent Bromine: An Advanced Redox Mediator For Rechargeable Lithium-Oxygen Batteries. *Chem. Commun.* **2022**, *58* (98), 13632−13635.
(83) Jeong, M. G.; Lee, H. H.; Shin, H. J.; Jeong, Y.; Hwang, J. Y.; Kwak, W. J.; Oh, G.; Kim, W.; Ryu, K.; Yu, S. H.; et al. A fluoroalkyl iodide additive for Li-O_2 battery electrolytes enables stable cycle life and high reversibility. *J. Mater. Chem. A* **2023**, *11* (28), 15246−15255.
(84) Wang, Q. Y.; Zheng, M. T.; Gao, M. L.; Liao, Y. L.; Zhang, X. P.; Fan, C.; Chen, W. R.; Lu, J. Simultaneously Generating Redox Mediator and Hybrid SEI for Lithium-oxygen Batteries by Lewis Acid Catalyzed Ring-opening Reaction of Organic Iodine. *Adv. Funct. Mater.* **2023**, DOI: 10.1002/adfm.202312723.
(85) Wang, X. F.; Li, Y. J.; Bi, X. X.; Ma, L.; Wu, T. P.; Sina, M.; Wang, S.; Zhang, M. H.; Alvarado, J.; Lu, B. Y.; et al. Hybrid Li-Ion and Li-O_2 Battery Enabled by Oxyhalogen-Sulfur Electrochemistry. *Joule* **2018**, *2* (11), 2381−2392.
(86) Zhang, J.; Sun, B.; Zhao, Y.; Kretschmer, K.; Wang, G. Modified Tetrathiafulvalene as an Organic Conductor for Improving Performances of Li-O_2 Batteries. *Angew. Chem. Int. Ed.* **2017**, *56* (29), 8505−8509.
(87) Wang, D.; Zhang, F.; He, P.; Zhou, H. A Versatile Halide Ester Enabling Li-Anode Stability and a High Rate Capability in Lithium-Oxygen Batteries. *Angew. Chem. Int. Ed.* **2019**, *58* (8), 2355−2359.
(88) Guo, Z.; Li, C.; Liu, J.; Wang, Y.; Xia, Y. A Long-Life Lithium-Air Battery in Ambient Air with a Polymer Electrolyte Containing a Redox Mediator. *Angew. Chem. Int. Ed.* **2017**, *56* (26), 7505−7509.
(89) Akella, S. H.; Bagavathi, M.; Rosy; Sharon, D.; Ozgur, C.; Noked, M. Exploring the Impact of Lithium Halide-Based Redox Mediators in Suppressing Co_2 Evolution In Li-O_2 Cells. *J. Mater. Chem. A* **2023**, *11* (38), 20480−20487.
(90) Gao, Z.; Temprano, I.; Lei, J.; Tang, L.; Li, J.; Grey, C. P.; Liu, T. Recent Progress in Developing a LiOH-Based Reversible Nonaqueous Lithium-Air Battery. *Adv. Mater.* **2023**, *35* (1), No. 2201384.
(91) Ling, C.; Zhang, R. G.; Takechi, K.; Mizuno, F. Intrinsic Barrier to Electrochemically Decompose Li_2CO_3 and LiOH. *J. Phys. Chem. C* **2014**, *118* (46), 26591−26598.
(92) Li, F.; Wu, S.; Li, D.; Zhang, T.; He, P.; Yamada, A.; Zhou, H. The Water Catalysis at Oxygen Cathodes of Lithium-Oxygen Cells. *Nat. Commun.* **2015**, *6*, 7843.
(93) Zhang, X.; Dong, P.; Noh, S.; Zhang, X.; Cha, Y.; Ha, S.; Jang, J. H.; Song, M. K. Unravelling the Complex LiOH-Based Cathode Chemistry in Lithium-Oxygen Batteries. *Angew. Chem. Int. Ed.* **2023**, *62* (4), No. e202212942.
(94) Liu, T.; Liu, Z.; Kim, G.; Frith, J. T.; Garcia-Araez, N.; Grey, C. P. Understanding LiOH Chemistry in a Ruthenium-Catalyzed Li-O_2 Battery. *Angew. Chem. Int. Ed.* **2017**, *56* (50), 16057−16062.
(95) Liu, Y.; Zhao, S.; Wang, D.; Chen, B.; Zhang, Z.; Sheng, J.; Zhong, X.; Zou, X.; Jiang, S. P.; Zhou, G.; et al. Toward an Understanding of the Reversible Li-CO_2 Batteries over Metal-N_4-Functionalized Graphene Electrocatalysts. *ACS Nano* **2022**, *16* (1), 1523−1532.
(96) Kwabi, D. G.; Batcho, T. P.; Amanchukwu, C. V.; Ortiz-Vitoriano, N.; Hammond, P.; Thompson, C. V.; Shao-Horn, Y. Chemical Instability of Dimethyl Sulfoxide in Lithium-Air Batteries. *J. Phys. Chem. Lett.* **2014**, *5* (16), 2850−2856.
(97) Zhu, Y. G.; Liu, Q.; Rong, Y.; Chen, H.; Yang, J.; Jia, C.; Yu, L. J.; Karton, A.; Ren, Y.; Xu, X.; et al. Proton enhanced dynamic battery chemistry for aprotic lithium-oxygen batteries. *Nat. Commun.* **2017**, *8*, 14308.
(98) Huang, K.; Wan, H.; Gong, Z.; Liu, J.; Yan, M.; Wu, J.; Cui, C.; Ye, G.; Reuter, K.; Fei, H. Cobalt Single Atom-Catalyzed Formation of LiOH in Li-O_2 Batteries via the Direct 4-Electron Oxygen Reduction Pathway. *CCS Chem.* **2024**, 1.
(99) Lu, J.; Dey, S.; Temprano, I.; Jin, Y.; Xu, C.; Shao, Y.; Grey, C. P. Co_3O_4-Catalyzed LiOH Chemistry in Li-O_2 Batteries. *ACS Energy Lett.* **2020**, *5* (12), 3681−3691.
(100) Bi, X.; Li, M.; Liu, C.; Yuan, Y.; Wang, H.; Key, B.; Wang, R.; Shahbazian-Yassar, R.; Curtiss, L. A.; Lu, J.; Amine, K. Cation Additive Enabled Rechargeable LiOH-Based Lithium-Oxygen Batteries. *Angew. Chem. Int. Ed.* **2020**, *59* (51), 22978−22982.
(101) Cui, C.; Yang, C.; Eidson, N.; Chen, J.; Han, F.; Chen, L.; Luo, C.; Wang, P. F.; Fan, X.; Wang, C. A Highly Reversible, Dendrite-Free Lithium Metal Anode Enabled by a Lithium-Fluoride-Enriched Interphase. *Adv. Mater.* **2020**, *32* (12), No. e1906427.
(102) Rastegar, S.; Hemmat, Z.; Zhang, C.; Plunkett, S.; Wen, J.; Dandu, N.; Rojas, T.; Majidi, L.; Misal, S. N.; Ngo, A. T.; et al. High-Rate Long Cycle-Life Li-Air Battery Aided by Bifunctional InX_3 (X = I and Br) Redox Mediators. *ACS Appl. Mater. Interfaces* **2021**, *13* (4), 4915−4922.
(103) Wang, L.; Li, W.; Sun, X.; Mu, X.; Sheng, C.; Wen, Z.; He, P.; Zhou, H. Trifunctional imidazolium bromide: a high-efficiency redox mediator for high-performance Li-O_2 batteries. *Chem. Commun.* **2023**, *59* (60), 9215−9218.
(104) Zhao, H. M.; Chi, Z. Z.; Kong, D. Z.; Li, L.; Tian, M. E.; Guo, Z. Y.; Wang, L. Constructing *In-Situ* $SOCl_2$-Induced Protective Layer on Li Anode for High-Performance Li-O_2 Batteries Containing LiI Redox Mediator. *Chem. Eng. J.* **2023**, *469*, 143962.
(105) Matsuda, S.; Kubo, Y.; Uosaki, K.; Hashimoto, K.; Nakanishi, S. Improved Energy Capacity of Aprotic Li-O2 Batteries by Forming Cl-Incorporated Li_2O_2 as the Discharge Product. *J. Phys. Chem. C* **2016**, *120* (25), 13360−13365.
(106) Kwak, W. J.; Park, S. J.; Jung, H. G.; Sun, Y. K. Optimized Concentration of Redox Mediator and Surface Protection of Li Metal for Maintenance of High Energy Efficiency in Li-O_2 Batteries. *Adv. Energy Mater.* **2018**, *8* (9), 1702258.
(107) Shi, L.; Wang, G.; Li, J.; Wu, M. F.; Wen, Z. Y. Sulfonated Bacterial Cellulose-Based Functional Gel Polymer Electrolyte for Li-O_2 Batteries with LiI as a Redox Mediator. *Acs Sustain. Chem. Eng.* **2021**, *9* (41), 13883−13892.
(108) Qiao, Y.; He, Y. B.; Wu, S. C.; Jiang, K. Z.; Li, X.; Guo, S. H.; He, P.; Zhou, H. S. MOF-Based Separator in an Li-O_2 Battery: An Effective Strategy to Restrain the Shuttling of Dual Redox Mediators. *ACS Energy Lett.* **2018**, *3* (2), 463−468.
(109) Ko, Y. M.; Kim, H. I.; Cho, S. J.; Lee, K. M.; Jung, G. Y.; Park, H. J.; Park, S. H.; Lee, Y. J.; Bae, Y. J.; Lee, Y. R. Liquid-Based Janus Electrolyte for Sustainable Redox Mediation in Lithium-Oxygen Batteries. *Adv. Energy Mater.* **2021**, *11* (38), 2102096.
(110) Wang, Y. F.; Song, L. N.; Li, F.; Wang, Y.; Wang, X. X.; Li, M. L.; Zou, L. C.; Xu, J. J. Enabling Shuttle-Free of High Concentration Redox Mediators by Metal Organic Framework Derivatives in Lithium-Oxygen Batteries. *J. Power Sources* **2021**, *492*, 229575.
(111) Zhang, X. P.; Li, Y. N.; Sun, Y. Y.; Zhang, T. Inverting the Triiodide Formation Reaction by the Synergy between Strong Electrolyte Solvation and Cathode Adsorption for Lithium-Oxygen Batteries. *Angew. Chem. Int. Ed.* **2019**, *58* (51), 18394−18398.
(112) Ito, K.; Matsumura, D.; Song, C.; Kubo, Y. Operando Br K-Edge Dispersive X-ray Absorption Fine Structure Analysis for Br^{-}/Br_3^{-} Redox Mediator for Li-Air Batteries. *ACS Energy Lett.* **2022**, *7* (6), 2024−2028.
(113) Torres, A. E.; Ramos, E.; Balbuena, P. B. LiOH Formation from Lithium Peroxide Clusters and the Role of Iodide Additive. *J. Phys. Chem. C* **2020**, *124* (19), 10280−10287.

(114) Freunberger, S. A.; Chen, Y.; Drewett, N. E.; Hardwick, L. J.; Barde, F.; Bruce, P. G. The Lithium-Oxygen Battery with Ether-Based Electrolytes. *Angew. Chem. Int. Ed.* **2011**, *50* (37), 8609−8613.
(115) Wang, A.; Wu, X.; Zou, Z.; Qiao, Y.; Wang, D.; Xing, L.; Chen, Y.; Lin, Y.; Avdeev, M.; Shi, S. The Origin of Solvent Deprotonation in LiI-added Aprotic Electrolytes for Li-O_2 Batteries. *Angew. Chem. Int. Ed.* **2023**, *62* (14), No. e202217354.
(116) Yu, Q.; Ye, S. In Situ Study of Oxygen Reduction in Dimethyl Sulfoxide (DMSO) Solution: A Fundamental Study for Development of the Lithium-Oxygen Battery. *J. Phys. Chem. C* **2015**, *119* (22), 12236−12250.
(117) Aetukuri, N. B.; McCloskey, B. D.; García, J. M.; Krupp, L. E.; Viswanathan, V.; Luntz, A. C. Solvating Additives Drive Solution-Mediated Electrochemistry and Enhance Toroid Growth in Non-Aqueous Li-O_2 Batteries. *Nat. Chem.* **2015**, *7* (1), 50−56.
(118) Liu, T.; Kim, G.; Jónsson, E.; Castillo-Martinez, E.; Temprano, I.; Shao, Y.; Carretero-González, J.; Kerber, R. N.; Grey, C. P. Understanding LiOH Formation in a Li-O_2 Battery with LiI and H_2O Additives. *ACS Catal.* **2019**, *9* (1), 66−77.
(119) Li, Y.; Dong, S.; Chen, B.; Lu, C.; Liu, K.; Zhang, Z.; Du, H.; Wang, X.; Chen, X.; Zhou, X.; et al. Li-O_2 Cell with LiI(3-hydroxypropionitrile)$_2$ as a Redox Mediator: Insight into the Working Mechanism of I^- during Charge in Anhydrous Systems. *J. Phys. Chem. Lett.* **2017**, *8* (17), 4218−4225.
(120) Kim, H.; Kwak, W. J.; Jung, H. G.; Sun, Y. K. Verification for Trihalide Ions as Redox Mediators in Li-O_2 Batteries. *Energy Stor. Mater.* **2019**, *19*, 148−153.
(121) Zhang, W.; Shen, Y.; Sun, D.; Huang, Z. M.; Zhou, J.; Yan, H.; Huang, Y. H. Promoting Li_2O_2 Oxidation via Solvent-Assisted Redox Shuttle Process for Low Overpotential Li-O_2 Battery. *Nano Energy* **2016**, *30*, 43−51.
(122) Viswanathan, V.; Pande, V.; Abraham, K. M.; Luntz, A. C.; McCloskey, B. D.; Addison, D. Comment On "Cycling Li-O_2 Batteries via LiOH Formation and Decomposition". *Science* **2016**, *352* (6286), 667.
(123) Shen, Y.; Zhang, W.; Chou, S. L.; Dou, S. X. Comment On "Cycling Li-O_2 Batteries via LiOH Formation and Decomposition". *Science* **2016**, *352* (6286), 667.
(124) Leverick, G.; Tulodziecki, M.; Tatara, R.; Bardé, F.; Shao-Horn, Y. Solvent-Dependent Oxidizing Power of LiI Redox Couples for Li-O_2 Batteries. *Joule* **2019**, *3* (4), 1106−1126.
(125) Leverick, G.; Feng, S.; Acosta, P.; Acquaviva, S.; Barde, F.; Cotte, S.; Shao-Horn, Y. Tunable Redox Mediators for Li-O_2 Batteries Based on Interhalide Complexes. *ACS Appl. Mater. Interfaces* **2022**, *14* (5), 6689−6701.
(126) Temprano, I.; Liu, T.; Petrucco, E.; Ellison, J. H. J.; Kim, G.; Jónsson, E.; Grey, C. P. Toward Reversible and Moisture-Tolerant Aprotic Lithium-Air Batteries. *Joule* **2020**, *4* (11), 2501−2520.
(127) Zhang, Q. K.; Zhang, X. Q.; Wan, J.; Yao, N.; Song, T. L.; Xie, J.; Hou, L. P.; Zhou, M. Y.; Chen, X.; Li, B. Q.; et al. Homogeneous and Mechanically Stable Solid-Electrolyte Interphase Enabled by Trioxane-Modulated Electrolytes for Lithium Metal Batteries. *Nat. Energy* **2023**, *8* (7), 725−735.
(128) Wu, X.; Wang, X.; Li, Z.; Chen, L.; Zhou, S.; Zhang, H.; Qiao, Y.; Yue, H.; Huang, L.; Sun, S. G. Stabilizing Li-O_2 Batteries with Multifunctional Fluorinated Graphene. *Nano Lett.* **2022**, *22* (12), 4985−4992.
(129) Li, D.; Xu, K.; Zhu, M.; Xu, T.; Fan, Z.; Zhu, L.; Zhu, Y. Synergistic Catalysis by Single-Atom Catalysts and Redox Mediator to Improve Lithium-Oxygen Batteries Performance. *Small* **2021**, *17* (38), No. 2101620.
(130) He, Y.; Ding, L.; Cheng, J.; Mei, S.; Xie, X.; Zheng, Z.; Pan, W.; Qin, Y.; Huang, F.; Peng, Y.; Deng, Z. A "Trinity" Design of Li-O_2 Battery Engaging the Slow-Release Capsule of Redox Mediators. *Adv. Mater.* **2023**, *35* (49), No. e2308134.
(131) Lai, J.; Xing, Y.; Chen, N.; Li, L.; Wu, F.; Chen, R. Electrolytes for Rechargeable Lithium-Air Batteries. *Angew. Chem. Int. Ed.* **2020**, *59* (8), 2974−2997.
(132) Li, Y.; Wang, X.; Dong, S.; Chen, X.; Cui, G. Recent Advances in Non-Aqueous Electrolyte for Rechargeable Li-O_2 Batteries. *Adv. Energy Mater.* **2016**, *6* (18), 1600751.
(133) Chen, Y.; Gao, X.; Johnson, L. R.; Bruce, P. G. Kinetics of Lithium Peroxide Oxidation by Redox Mediators and Consequences for the Lithium-Oxygen Cell. *Nat. Commun.* **2018**, *9* (1), 767.
(134) Ahn, S.; Zor, C.; Yang, S.; Lagnoni, M.; Dewar, D.; Nimmo, T.; Chau, C.; Jenkins, M.; Kibler, A. J.; Pateman, A.; et al. Why Charging Li-Air Batteries with Current Low-Voltage Mediators Is Slow and Singlet Oxygen Does Not Explain Degradation. *Nat. Chem.* **2023**, *15* (7), 1022−1029.

https://doi.org/10.1021/cbe.4c00025
Chem Bio Eng. 2024, 1, 737−756